UNIVERSITY OF OKLAHOMA

GRADUATE COLLEGE

Evaluation of Flash Drought Criteria Components

A THESIS

SUBMITTED TO THE GRADUATE FACULTY

in partial fulfillment of the requirements for the

Degree of

Master of Science in Meteorology

By

Stuart Edris

Norman, Oklahoma

2020

Evaluation of Flash Drought Criteria Components

A THESIS APPROVED FOR THE

School of Meteorology

BY THE COMMITTEE CONSISTING OF

Dr. Jeffrey B. Basara, Chair

Dr. Bradley G. Illston

Dr. Scott T. Salesky

Acknowledgements

The author would like to acknowledge and thank his advisor Dr. Jeff Basara, for proposing the project idea, providing continuous feedback, having a great deal of patience when the writing process was slow (to nonexistent at times), and continually helping to edit the paper as it progressed. Additional thanks goes one of the collaborators for the project, Dr. Jordan Christian, for continuous feedback, assistance in collecting the data for this project, and help in debugging the codework as it progressed. The author would also like to thank the other collaborators Ryann Wakefield and Dr. Brad Illston for their support and feedback as the project developed. Finally, the author would like to thank the committee for their support and willingness to help.

The author would also like to acknowledge the grants used to sponsor and support this project. This work was supported, in part, by the NOAA Climate Program Office's Sectoral Applications Research Program (SARP) Grant NA130AR4310122, the Agriculture and Food Research Initative Competitive Grant no. 2012-02355, from the USDA National Institute of Food and Agriculture, the USDA National Institute of Food and Agriculture (NIFA) Grant no 2016-6800224967, the NASA Water Resources Program Grant 80NSSC19K1266, and the USDA Southern Great Plains Climate Hub.

Table of Contents

Abstract

Flash droughts occur rapidly (~1 month timescale) and have produced significant ecological, agricultural, and socioeconomical impacts. Recent advances in our understanding of flash droughts have resulted in methods to identify and quantify flash drought events. However, little work has been done to isolate the individual flash (or rapid intensification) and drought components of flash drought, which could further determine their cause, evolution, and predictability. As such, this study utilized a flash drought identification method developed by Christian et al. (2019) to quantify individual components of flash drought through 1979 – 2019, using evapotranspiration (ET) and potential evapotranspiration (PET) data from the North American Regional Reanalysis Model (NARR). Flash droughts were identified using the standardized evaporative stress ratio (SESR), which uses four criteria to identify flash droughts: (1) the flash drought lasts at least 30 days, (2) SESR is below the 20th percentile at the end of the rapid intensification, (3) standardized changes in SESR on the pentad timescale is below the 40th percentile, and (4) the mean standardized change in SESR for the entire flash drought is below the 25th percentile. Because the first, third, and fourth criteria involve checks for rapid drying or rapid intensification of drought they are used to represent the rapid intensification or "flash" component of flash drought. The drought component (represented by criteria 2) was assessed using the U.S. Drought Monitor for 2010 – 2019 and individual case studies were examined, and the flash component was assessed using results of previous flash drought studies. In addition, the correlation coefficient and composite mean difference was calculated between the flash component and flash droughts identified to determine what regions, if any, experienced rapid intensification but did not fall into flash drought. The results yielded that SESR was able to represent the spatial coverage of drought well for regions east of the Rocky Mountains, with mixed success regarding the intensity of the drought events.

The flash component tended to agree well with other flash drought studies, though it is more challenging to verify as no other measure of rapid drying is available for cross validation. Further, the overall climatology of the flash component showed similar hotspots to the flash drought climatology east of the Rocky Mountains, but also suggested areas west of the Rocky Mountains experience rapid intensification at high frequencies.

1. Introduction

Drought is a climate extreme resulting from below normal precipitation over a prolonged period of time, which causes an imbalance in the hydrologic system (American Meteorological Society 1997; Pachauri et al. 2014). This puts stress on ecological systems and can have large socioeconomic impacts, and extreme events can cost over 10 billion dollars losses (Heim 2002; Dai 2011; NCEI 2017). Many studies, therefore, have focused on being able detect, monitor, and predict drought events. Historically, this has been done through long term indices (∼2 - 6+ month averages) such as the Palmer Drought Severity Index (PDSI) and Standardized Precipitation Index (SPI). However, more recent studies have focused on drought events that undergo rapid evolution (over ∼1 month), coined "flash drought" in Svoboda et al. (2002). These flash droughts differ from the more traditional seasonal to subseasonal droughts in several ways. While traditional drought can occur in any given season, flash drought has a distinct seasonality, favoring the spring and summer seasons (Chen et al. 2019; Christian et al. 2019; Noguera et al. 2020). Additionally, traditional drought can occur in any given region, while flash droughts tend to favor transition zones with a strong precipitation gradient in the climatology and regions where the terrestrial land is strongly coupled with the atmosphere (Kim and Rhee 2016; Chen et al. 2019; Christian et al. 2019; Wakefield et al. 2019). Further, because of the rapid drying and desiccation of the terrestrial surface, flash droughts can have a large ecological, agricultural, and socioeconomic impacts (e.g., the 2012 flash drought had numerous impacts on agriculture; Otkin et al. 2015, 2018; Basara et al. 2019).

Because flash droughts occur over short time periods, traditional drought monitoring, evaluation, and detection methods are generally unable to accurately capture flash drought and rapid intensification events. As such, there has been significant work focused on variables that respond to a rapidly drying environment and that can be updated quickly (~ 1 week timescale) and can thus detect rapid onset of drought on shorter time scales, such as soil moisture (e.g. Hunt et al. 2009; Ford et al. 2015; Otkin et al. 2019; Liu et al. 2020) and evapotranspiration (ET) and potential evapotranspiration (PET; e.g., Otkin et al. 2013, 2014; Li et al. 2020; Kim et al. 2019; Hobbins et al. 2016; McEvoy et al. 2016; Kim et al. 2019; Vicente-Serrano et al. 2018; Christian et al. 2019). In particular, ET has been found to be one of the most sensitive variables to flash drought with the fastest decline rates during rapid intensification events, and thus, it serves as a precursor for flash drought development, typically about 1 – 2 weeks in advance (Otkin et al. 2013; Chen et al. 2019). In addition, ET has been associated with the atmospheric supply of moisture available to the environment while PET is associated with the terrestrial demand for moisture (Hobbins et al. 2016; Christian et al. 2019). As such, many studies have focused on ET and PET, creating a number of standardized indices to measure drought such as the evaporative demand drought index (EDDI; Hobbins et al. 2016; McEvoy et al. 2016), the standardized evapotranspiration deficit index (Kim and Rhee 2016; Kim et al. 2019), the evaporative stress index (ESI; Otkin et al. 2013), the rapid change index (RCI; Otkin et al. 2014), and the standardized evaporative stress ratio (SESR; Christian et al. 2019). Further, ET is able to not only describe flash drought events, but it can also be used to examine drought in general, and capture historic drought events (Kim and Rhee 2016; Kim et al. 2019).

With the addition of numerous studies examining flash droughts events and the creation of numerous indices to identify and quantify flash drought events, Otkin et al. (2018) proposed creating a concrete definition for flash drought that required that any flash drought definition focus on two components for it. First, a "flash" or rapid intensification component to quantify rapid drying over a period on the order of a month should be included as the ability to identify rapid intensification. This is potentially the most critical part in identifying flash drought given its importance in flash drought development (Liu et al. 2020; Noguera et al. 2020) and impacts due to rapid desiccation of the terrestrial surface. Additionally, a drought component should be clearly identifiable (drought conditions must be met whereby environment discriminators are below the 20^{th} percentile).

Several studies have worked to quantify flash droughts events, using the United States Drought Monitor (USDM) database (Chen et al. 2019), soil moisture (Liu et al. 2020), SESR (Christian et al. 2019), and the standardized evaporative precipitation index (SPEI) at a monthly timescale (Noguera et al. 2020). Of particular interest is the flash drought identification method by Christian et al. (2019). This method has a number of benefits in that it can be applied to any gridded system. Additionally, it can be used to identify flash drought and its components in real time or predictively, so long as the dataset used is in real time or predictive. This method uses four separate criteria that determine the flash and drought components individually. Dividing flash droughts into these two components can be critical in determining several features associated with flash drought events. For example, quantifying the climatology of the rapid intensification can help improve understanding of flash droughts drivers, aid in their real time

identification, and identify areas to improve the predictability of flash droughts. At the same time, few studies have examined the individual components of flash droughts separately. As such, this study utilizes the method of identifying flash drought introduced within Christian et al. (2019) to analyze the flash and drought components individually. The climatology of rapid intensification (i.e., the "flash" component) is determined and the prominence of each component on flash drought development is explored for different regions across the United States (U.S.) compared to the USDM.

2. Data and Methods

a. Data

This study utilized data from the North American Regional Reanalysis (NARR) model which was designed to accurately represent the climate and hydrology of North America (Mesinger et al. 2006). The resolution of the NARR is 32 km × 32 km with a 3-hour temporal interval. For this study, surface evapotranspiration (ET) and potential evapotranspiration (PET) for the period spanning 1 January 1979 to 31 December 2019 (leap days were excluded for simplicity) were the critical variables incorporated into the analysis. PET was calculated within the Noah land surface model using the Penman equation with surface temperature, soil flux, radiation, windspeed, and specific humidity (Mesinger et al. 2006; Mahrt and Ek 1984). ET was composed of three components (evaporation from the soil, transpiration, and evaporation from canopy intercept),

which are calculated separately and then summed to obtain the total ET (Ek et al. 2003; Chen et al. 1996). The ET calculations incorporate numerous moisture and vegetation variables (vegetation density, stomatal conductance, precipitation, soil moisture, etc.).

The USDM is a collaboration between the National Drought Mitigation Center at the University of Nebraska-Lincoln, the U.S. Department of Agriculture, and the National Oceanic and Atmospheric Administration designed to monitor, identify, and convey information about drought to the public and stakeholders. It employs the use of numerous metrics (e.g., temperature, precipitation, streamflow, soil moisture, snowpack, ground water, and vegetation conditions) as well as professional opinions of the expert scientists who serve as drought monitor authors (Svoboda et al. 2002). Because the USDM is regarded as an accurate measure of drought identification, USDM drought values were incorporated into this study in order for testing and verification purposes. Because the data from the USDM are in a polygon format, it was rasterized in this study by comparing each grid point in the NARR grid to the polygon, and assigning the grid point the value of the polygon, similar to the method used in Chen et al. (2019). The values assigned for this study was 1 for D1 drought, 2 for D2, 3 for D3, and 4 for D4. Because this study was not concerned with abnormally dry events, D0 drought was given the same value as non drought conditions, which is 0. In addition, the USDM provides a basis for categorizing drought intensity based on percentiles (i.e., Table 2 in Svoboda et al. (2002)). Finally, when compared to the USDM, the SESR drought component was averaged to the same weekly time scale as the USDM. Because a level of subjectivity is incorporated into the USDM, proper consideration should be incorporated when compared to purely quantitative

methods (Leasor et al. 2020). In this case, because SESR responds more rapidly to changing conditions, which can make drought conditions vary week to week, and the USDM is more consistent due to the use an ensemble of variables over longer time scales, the performance of SESR is likely to be underestimated by the comparisons made here.

b. Standardized Evaporative Stress Ratio

This study employs the flash drought identification method developed by Christian et al. (2019), which incorporates surface moisture flux via ET (evaporation from the soil and transpiration from vegetation) along with the PET. These provide a measure of atmospheric demand for moisture, and it is dependent on the dryness of the terrestrial surface as well as the atmosphere. The ratio of ET to PET yields the evaporative stress ratio (ESR) defined in Christian et al. (2019) as:

$$ESR = \frac{ET}{PET} \tag{1}$$

whereby ESR values range from 0 (a completely dry near-surface atmosphere) to 1 (a saturated near-surface atmosphere). Due to the diurnal variability of ESR, it is recommended to use ESR on a daily mean values of ESR or pentad time scales (Christian et al. 2019); this study utilized the pentad time scale similar to Christian et al. (2019). The pentads used in this study were 5 day, non-overlapping averages.

To better investigate flash droughts events across different climate zones, the standardized evaporative stress ratio (SESR) was used.

$$SESR_{ijp} = \frac{ESR_{ijp} - \overline{ESR_{ijp}}}{\sigma_{ESR_{ijp}}} \quad (2)$$

The subscripts *i* and *j* refer to the i^{th} and j^{th} grid point and the subscript *p* refers to the p^{th} pentad in the Gregorian calendar (leap days excluded). Overbars indicate means values, and σ refers to standard deviations. For this study, the mean and standard deviation values were calculated from the 41 years in the dataset. Negative values of SESR indicate a region is drier than normal, and a region is more moist than normal when SESR is positive. Changes in SESR were also computed to determine how SESR changes in time (whether the region is drying or moistening in time). The change in SESR is given by

$$\Delta SESR_{ij,p} = SESR_{ij,p+1} - SESR_{ij,p} \quad (3)$$

where the subscript *p* indicates the p^{th} pentad. Note that ΔSESR should be calculated on the pentad timescale to better capture the trend in how SESR is changing. Note also that, for this study, the change in ΔSESR begins on the p^{th} pentad. Thus, if a grid has drying or moistening, it begins on the p^{th} pentad and ends on the $(p+1)^{th}$ pentad. Lastly, ΔSESR was also standardized before being used for the criteria analysis.

$$\left(\Delta SESR_{ijp}\right)_z = \frac{\Delta SESR_{ijp} - \overline{\Delta SESR_{ijp}}}{\sigma_{\Delta SESR_{ijp}}} \quad (4)$$

Here the subscript z indicates that $\Delta SESR$ is standardized (i.e., it is a z-score). Finally, the evaporative demand decreases exponentially in cold environments such that SESR becomes ill

defined to identify flash droughts in such conditions. As such, this study is restricted to the agricultural growing season (April – October), to focus on the favored season for flash droughts and similar to previous studies (Otkin et al. 2014; Chen et al. 2019; Christian et al. 2019; Noguera et al. 2020), with the domain set as the contiguous United States (CONUS).

c. Criteria Analysis

Christian et al. (2019) developed a method to identify flash drought for any gridded dataset using SESR. This method is based on four separate criteria, which are used to identify rapid drying and drought conditions separately. They are:

1. The flash drought must be at least 30 days in length.
2. At the end of the flash drought, the SESR value must be at or below the 20^{th} percentile for that grid point and pentad.
3.
    a) During the flash drought, $(\Delta SESR)_z$ must be at or below the 40^{th} percentile for that grid point and pentad.
    b) No more than one (1) exception is allowed for criteria 3a during the flash drought.
4. The mean change in $(\Delta SESR)_z$ during the whole flash drought must be at or below the 25^{th} percentile for that grid point and range of pentads.

Note that pentads (or means over larger time scales) are required for Criteria 3 and 4 because of the variability of SESR on smaller time scales, whereas Criteria 3 and 4 are more concerned with the general trend in SESR. For this study, each criterion was determined for each pentad in the dataset. To accomplish this, each day was treated as an "end date" for the flash drought. For each criteria analysis, a binary value of 1 (true, the criteria was satisfied for that pentad and grid point) or 0 (the criteria was not satisfied for that pentad and grid point) was given to each grid point and for each pentad, illustrated in Figure 1 and is described in more detail in the following sections. How these criteria identify flash drought is illustrated in Figure 2. A benefit of using the binary values is that the areal coverage of each component can be easily calculated by summing over all the grid points in a domain (at any time scale desired, such as pentad, weekly, monthly, or yearly), and multiplying by the areal coverage of each grid point (32 km × 32 km for the NARR grid). To make the results of this study more comparable with Christian et al. (2019), an offset of $100/2N_{year}$ was applied, where N_{year} is the number of years in the dataset, to account for differences in percentile calculations between MatLab and Python. Python has a higher percentile estimate, so the offset was subtracted if a percentile was estimated from a population, and added if a value was estimated for a given percentile.

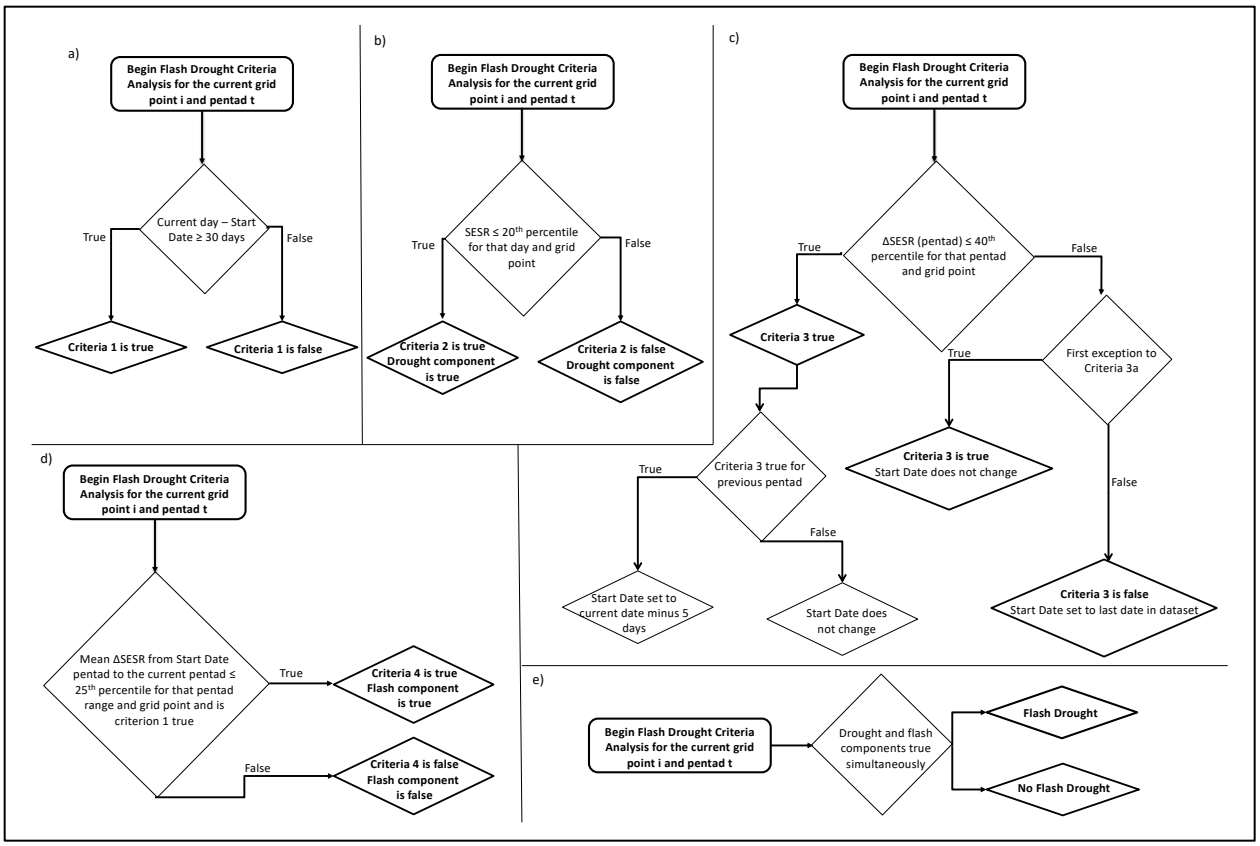

Figure 1. Flow Chart showing algorithm used for this study and how it calculated a) Criteria 1, b) Criteria 2 and the drought component, c) Criteria 3 and the Start Date, d) Criteria 4 and the flash component, and e) flash drought. The initial value for the Start Date was the last date in the data set, and Criteria 3 was initially assumed false.

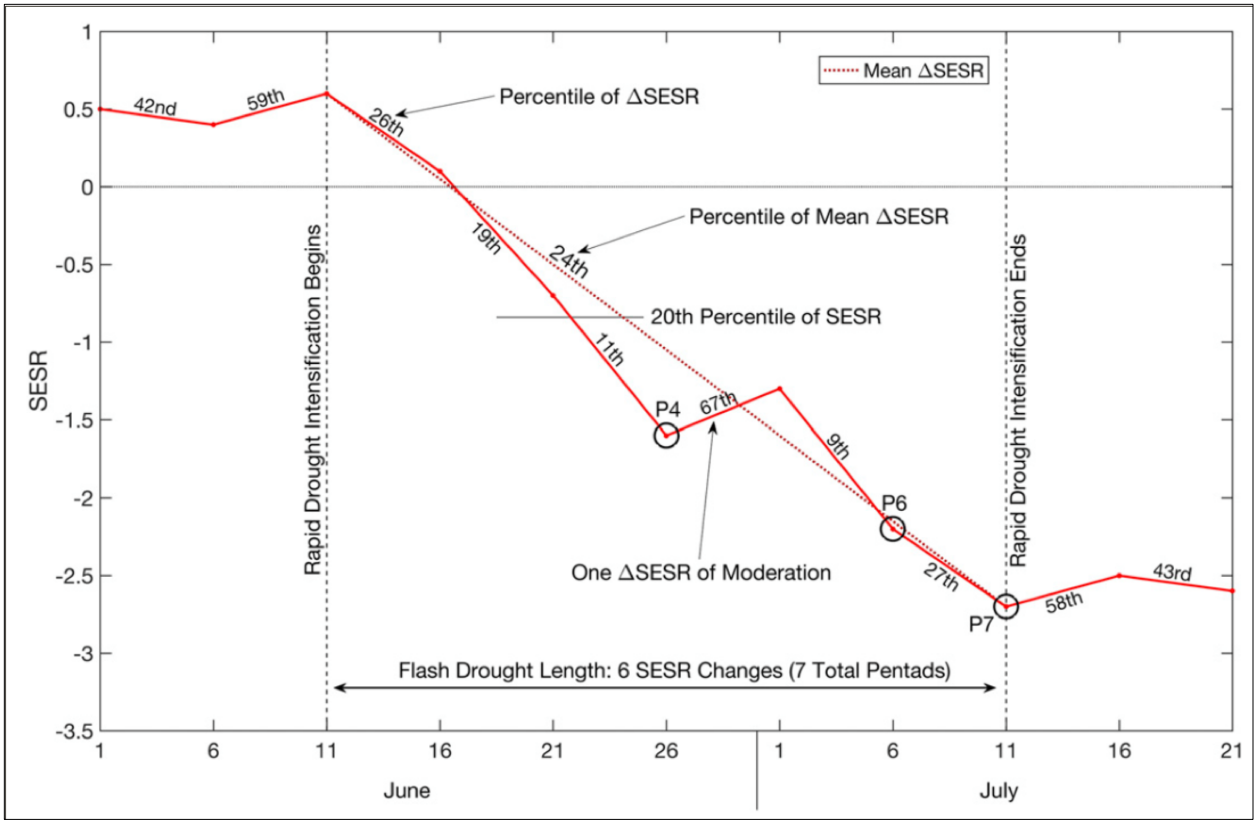

Figure 2. A time series schematic illustrating the four criteria used in the flash drought identification method. [Figure and caption from Figure 2 in Christian et al. 2019.]

1) Criteria 1

Physically, Criteria 1 is used to prevent the overall flash drought algorithm from identifying short-term "dry spells" as flash droughts. The algorithm checks whether the difference between the current day (plus five days, because criteria 3 considers $(\Delta SESR)_z$ which ends on the $(p+1)^{th}$ pentad) in the algorithm and the Start Date variable is greater than 30 days. If it is, Criteria 1 is true, and false otherwise. However, because the Start Date is set to a high value whenever Criteria 3 is false, then Criteria 1 is false whenever Criteria 3 is false (physically, no rapid

drying; computationally, because the difference in dates becomes negative). This means that Criteria 1 is only true whenever rapid drying has continuously occurred for at least 30 days. Note also that the algorithm only identifies continuous rapid drying at the end of a specific drying period. This is illustrated in Figure 2, where the flash drought identified was 30 days in length (from June 11 to July 11).

2) Criteria 2

Criteria 2 is potentially the simplest of the criteria to determine and interpret. For flash drought to occur, the variable being used to identify it must be below the 20^{th} percentile for that region and day to be considered in drought (Svoboda et al. 2002; Otkin et al. 2018). As such, Criteria 2 satisfies that requirement.

3) Criteria 3

Criteria 3 is a criterion that checks for rapid drying over a grid point. For a standardized variable, the 50^{th} percentile is approximately 0 (that is, 50% of the data should be below the mean, which is 0). As such, requiring that $(\Delta SESR)_z$ be at or below the 40^{th} percentile means this criterion is checking whether SESR is decreasing at a persistent pace within a pentad. Even so, Criteria 3 allows an exception in the event moderation of evaporative stress occurs during the flash drought development. For example, if a singular precipitation event occurs over a grid point experiencing flash drought, the precipitation could moderate the rate SESR decreases (or even

make it increase), but not enough to prevent the flash drought from occurring over the subseasonal period. Further, because this criterion identifies rapid drying from pentad to pentad, it can be used to determine when the flash drought begins and ends. This can be seen in the example shown in Figure 2. Note in that example, the flash drought is defined to begin when the rapid drying begins (i.e., when Criteria 3 is first true), and end when Criteria 3 is no longer true, with a single exception in the rapid drying allowed.

First, the algorithm determines if $(\Delta SESR)_z$ is at or below the 40^{th} percentile for that grid point and pentad p. If this is the case, then Criteria 3 is true for all days within the p^{th} pentad (because the decrease in SESR began within the pentad). An extra step is then implemented to determine if Criteria 3 is true or false for the previous pentad (that is, the $(p\text{-}1)^{th}$ pentad; it is assumed to be false for the first time step in the algorithm). If it is false, the algorithm assumes a flash drought is starting and sets a new variable (called Start Date in the algorithm) to the current day the algorithm is analyzing. If Criteria 3 is true for the previous pentad, then it determines there is already a flash drought developing and leaves Start Date unchanged. If $(\Delta SESR)_z$ is above the 40^{th} percentile, then the algorithm checks if this is the first exception in a flash drought. If it is, Criteria 3 is true and the Start Date is unchanged. If it is false, then Criteria 3 is set to false, and Start Date is set to the last date in the dataset (in this case, the very end of the NARR dataset; Start Date is initialized to the last date at the start of the algorithm as well). If no flash drought is determined, then the previous pentad has already failed Criteria 3a, so this second check will set Criteria 3 to false for this pentad, and following pentads until $(\Delta SESR)_z$ is below the 40^{th} percentile again.

4) Criteria 4

Criteria 4 is the second criteria designed to examine whether rapid drying that may be occurring over a grid point. Specifically, this criterion checks the overall drying between the start and end of the rapid drying period and determines if it was large enough to be considered a flash drought. This is accomplished within the algorithm by checking if the average of $(\Delta SESR)_z$ within the flash drought (that is, the pentads included between the start and end dates of the flash drought) is below the 25th percentile of that same mean for all years. An example of this is shown in Figure 2, where the mean in $(\Delta SESR)_z$ (dashed red line) is below the 25th percentile. Note that like Criteria 1 and 3, this criterion identifies the rapid drying at the end of the drying period. Further, like Criteria 1, Criteria 4 is always false when there is no rapid drying (if Start Date is after the current day in the algorithm, the mean becomes the mean of an empty vector and Criteria 4 defaults to false). Note that because each pentad is treated as an end date, some of the true or false values in Criteria 4 may be skewed to occur more frequently. This is because the mean of $(\Delta SESR)_z$ may occur over time periods less than 30 days. For example, in Figure 2 flash drought starts at June 11. The algorithm would compute the mean change in SESR between the June 11 – June 16 pentads, between the June 11 – June 21 pentads, and so on which may be easier to pass than full 30 day average. The algorithm accounts for this by requiring Criteria 1 to be true for Criteria 4 to be true. In this way, it is ensured all mean values are over 30 days or more. Note this also dictates that Criteria 4 depends on Criteria 1 and 3 (both of which measure rapid drying components).

d. Flash and Drought Components

A critical aspect of this study was to more explicitly determine how well SESR can represent drought in general, both in spatial coverage and in intensity. Drought was identified and classified using SESR percentiles and the classification method provided by the USDM (Table 1). In addition, the spatial coverage of drought, or the drought component, is represented by Criteria 2. The remaining three criteria deal with rapid drying, or intensification in which Criteria 3 searches for rapid drying, Criteria 1 uses this to identify rapid drying over longer periods, and Criteria 4 checks whether the magnitude of drying was rapid enough to be considered as rapid intensification. Overall, Criteria 4 can be used to represent Criteria 1 and 3, because it is only true when both are true. Because Criteria 4 also has its own check for rapid intensification, it represents all the components of rapid intensification and as such, the flash component of flash drought can be directly identified using Criteria 4.

Table 1. Percentiles used to determine drought categories with SESR. Percentiles are based on percentiles used in the U.S. Drought Monitor.

Drought Category	Percentile Range
No Drought	21 – 100
Category 1	11 – 20
Category 2	6 – 10
Category 3	3 – 5
Category 4	< 2

e. Statistical Analysis

Statistical comparisons were performed to quantify (1) areas that experienced rapid intensification, but did not yield flash drought, as well as (2) to compare the drought component to the USDM. These comparisons were accomplished by calculating the correlation coefficient and composite mean difference (mean in time). The correlation coefficient ® and composite mean difference (CD) equations used in this study were:

$$r_{ij} = \frac{\overline{x'_{ij} y'_{ij}}}{\overline{x'_{ij}}\,\overline{y'_{ij}}} \tag{5}$$

$$CD_{ij} = \overline{x_{ij}} - \overline{y_{ij}} \tag{6}$$

Where the overbar indicates a mean in time and a prime indicates a deviation (e.g., $x' = x - \bar{x}$). Subscripts *i* and *j* refer to the i^{th} and j^{th} grid point. For this project, *x* is either the SESR flash component or the SESR drought component. If *x* is the flash component, then *y* is the flash drought identified. If *x* is the drought component, then *y* is the USDM drought identified. Statistical significance was calculated by using the Monte-Carlo method with N = 5000.

If the correlation coefficient between the SESR flash component and flash drought is at or near 1, then they are well correlated and rapid intensification is a dominant factor in the occurrence of flash drought over that grid point. Conversely, if the correlation coefficient is near 0, then the rapid intensification events occur without flash drought (flash drought requires rapid

intensification *and* drought). Hence, correlations near 0 can be used to identify regions that experience rapid intensification but not drought. The same information is given by the composite mean difference. If the number of rapid intensification and flash droughts are the same, then their composite difference is near 0. If there is rapid intensification without flash drought, then their composite difference should be greater than 0.

In addition, these statistical methods were also used to compare the SESR drought component with the USDM. In this case, a correlation of 1 means a perfect comparison. That is, SESR perfectly predicts the USDM drought categories. A correlation of 0 indicates that SESR does not describe the USDM drought. The two may randomly agree (e.g., SESR may give the same drought intensity as the USDM), but this would not happen frequently enough to indicate correlation. In comparison, a correlation of -1 indicates that SESR and the USDM are oppositely correlated. That is, SESR has no drought when the USDM has drought and vice versa. Next, a composite mean of 0 is desired (the SESR drought component successfully identifies drought) and deviations from these gives increasingly worse identification results. Because the composite mean is the SESR drought component minus the USDM, then positive values indicate that SESR predicted either stronger drought than the USDM, more frequent drought than the USDM (that is, it had more weeks with drought than the USDM), or it predicted false positives (SESR predicted drought where there is none). Conversely, if the composite mean is negative, then SESR either underpredicted the strength of the drought, the frequency of the drought (that is, it had weeks where there was no drought), or SESR failed to predict drought where it should have (misses).

3. Case Studies

To examine the performance of the algorithm and to compare the drought component with the USDM for specific flash drought events, several years were chosen for further analysis. First, 2011 and 2012 were chosen because they have been widely reviewed and are well-studied events (e.g., for 2011 see Otkin et al. 2013; Ford et al. 2015; McEvoy et al. 2016; and Vicente-Serrano et al. 2018; for 2012 see Otkin et al. 2014; McEvoy et al. 2016; and Basara et al. 2019). In addition, a null year (2019) with weak drought was chosen to ensure the algorithm performed appropriately with null events as well as the extreme cases. Two additional years prior to 2010 (1988 and 2003) were also examined to examine how SESR represented these historic cases and to determine the utility of this algorithm to be able to describe drought events during the early stages of the USDM development as well as prior to the existence of the USDM.

a. 2011: Southern United States

During 2011, widespread and severe drought rapidly spread across much of the southern U.S. during the growing season, with the largest impacts focused on Texas and Oklahoma (Otkin et al. 2013; Ford et al. 2015; McEvoy et al. 2016; Vicente-Serrano et al. 2018). Figures 3 and 4 show the correlation and composite mean difference between the drought component and USDM. Overall, SESR was well correlated with the drought identified by the USDM, with the

correlation being statistically significant in most places except Texas. Additionally, some disagreement existed across Georgia, Texas, and locations further west, whereby the intensity was underestimated. This was because the composite difference for drought intensity is more negative than if just coverage is considered, implying SESR underestimated the intensity of the drought. However, based on Figure 5and some of the work by Vicente-Serrano et al. (2018), SESR seems to capture the spatial coverage of drought effectively (Supplementary Figure 1). However, the composite difference for spatial coverage of drought in Figure 4 is negative. Thus, SESR identified drought less frequently than the USDM. That is, there were weeks where SESR may not have identified drought, possibly due to some moderating influences, whereas there was the USDM recorded very persistent drought, giving the net negative difference in the spatial coverage comparison.

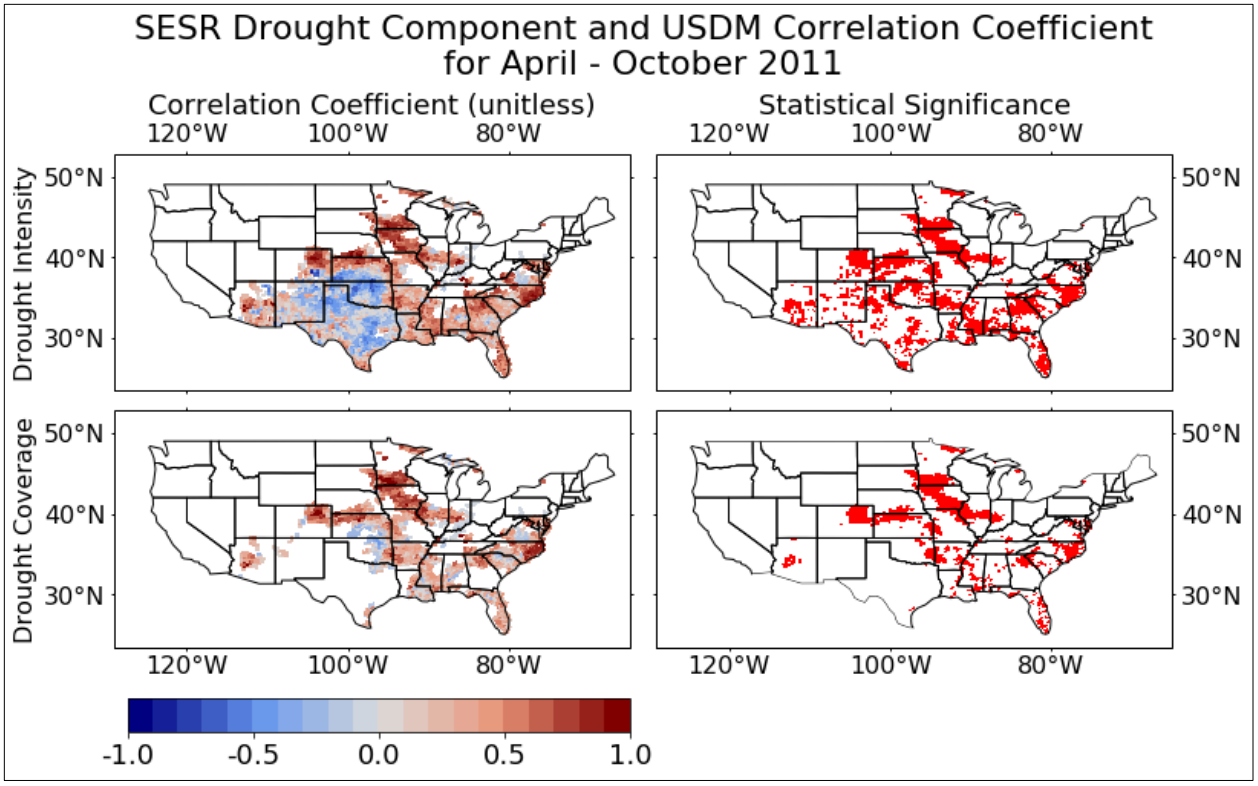

Figure 3. Correlation coefficient of the SESR drought component with the USDM for the growing season of 2011. (left) Correlation coefficient between the SESR drought component and USDM, and (right) the 95% statistical significance, calculated using the Monte-Carlo method with N = 5000. Statistical comparisons are for (top) drought coverage and intensity and (bottom) only drought coverage.

Figure 5 shows the general evolution of the drought component (left), flash component (center) and flash drought (right) for the growing season. In general, SESR yielded drought spread through most of west Texas and Louisiana in May, with expansion across most of the Deep South through most of June and July. SESR identified exceptional drought for west Texas and Louisiana, but not to the extend identified by the USDM. This would explain the low correlation,

as the USDM had exceptional drought for most of the state of Texas and the majority of the Deep South, and D3 in Georgia. Thus, it seems SESR did not identify some of the more extreme cases of drought during 2011. However, SESR did capture the spatial coverage of drought and was in strong agreement with other studies (Otkin et al. 2013; Kim and Rhee 2016; McEvoy et al. 2016; Vicente-Serrano et al. 2018) and it identified regions where the drought was most intense (though not necessarily the scale of the intensity).

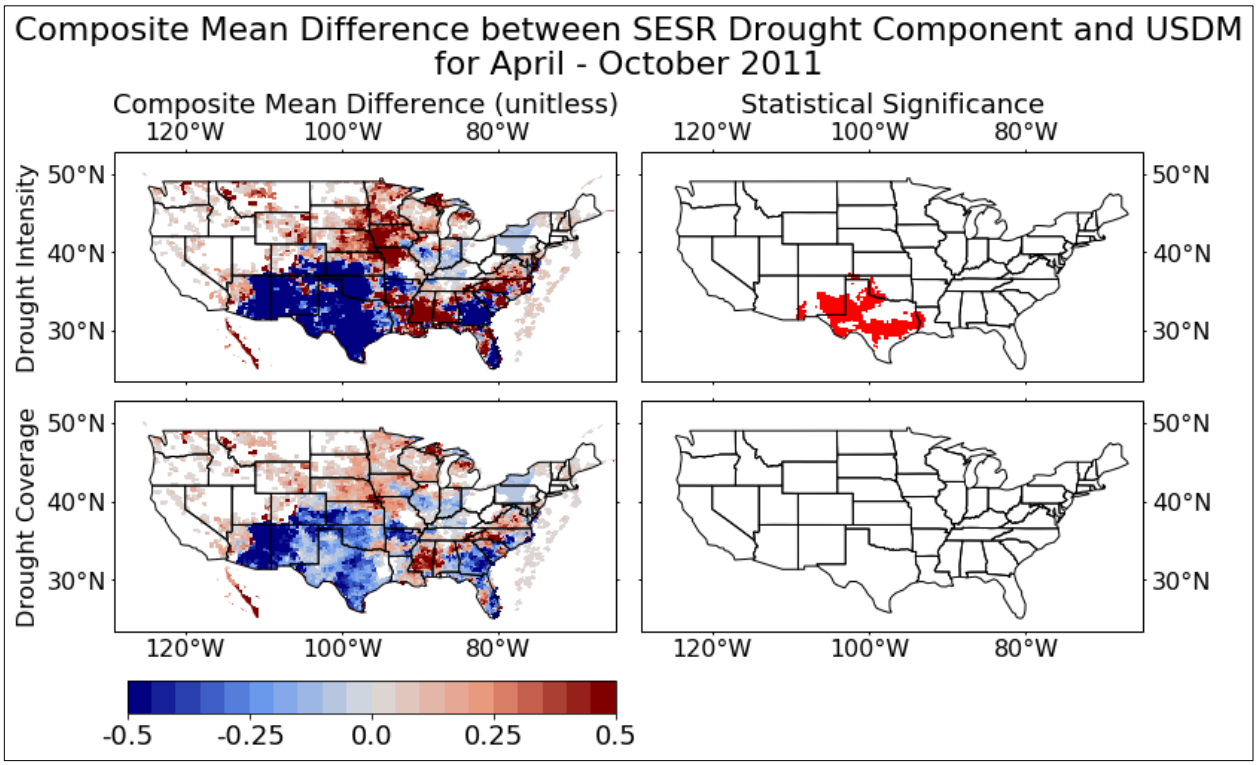

Figure 4. Composite mean difference between the SESR drought component and the USDM for the growing season of 2011. (left) Composite mean difference between the SESR drought component and the USDM, and (right) the 95% statistical significance, calculated using the Monte-Carlo method with N = 5000. Statistical comparisons are for (top) drought coverage and intensity and (bottom) only drought coverage.

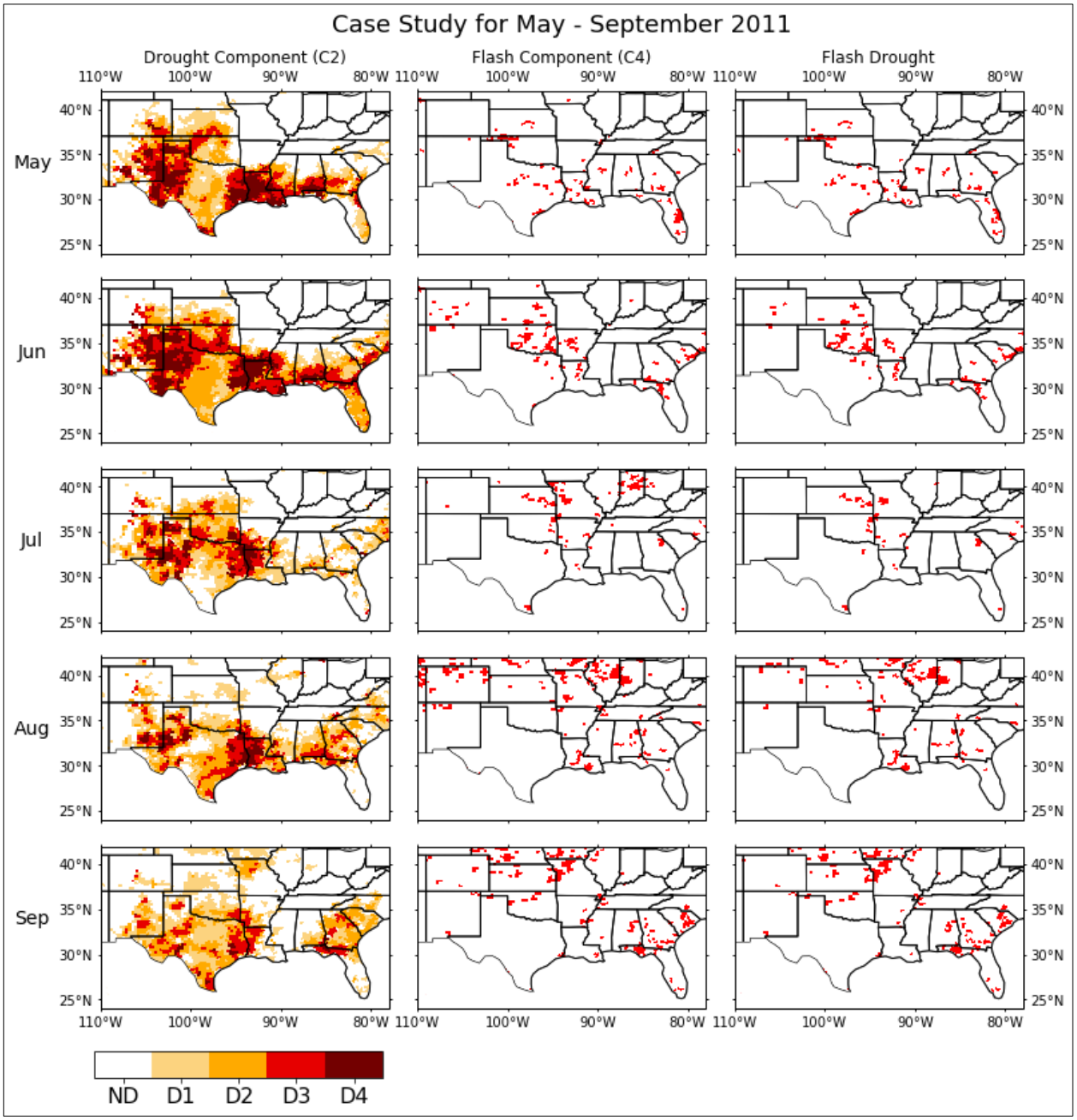

Figure 5. Case study for the growing season of 2011 (excluding March, April, and October). (left) Monthly average drought component (coverage and intensity), (center) monthly coverage of the SESR flash component, and (right) monthly coverage of flash drought. Red color indicates SESR flash component/drought was newly identified for at least 1 pentad in that month.

In terms of rapid intensification during 2011, SESR identified the areas of flash drought in parts of Texas and Oklahoma during May of 2011 that spread in that region during June, and propagated to the northeast as time progressed into August and September. In general, the identification of rapid intensification in central Oklahoma and north central Texas agrees with other studies (Otkin et al. 2013; Ford et al. 2015; McEvoy et al. 2016). The timing of flash drought identified in May with additional intensification events in June also agreed with results of previous studies (McEvoy et al. 2016). Overall, SESR successfully identified rapidly drying conditions in central Oklahoma and north central Texas during April into May. Little intensification occurred during May and early June in eastern Oklahoma and Arkansas due to some moderating precipitation events, but the dry conditions expanded in June and July and propagated north and east in the following months into the Corn Belt area, agreeing with the results of Flanagan et al. (2017).

b. 2012: Central and Midwestern United States

During 2012, a large and severe drought event spread across the Central U.S. with large impacts on the Corn Belt, and upper Mississippi River (Otkin et al. 2014; Ford et al. 2015; McEvoy et al. 2016; Basara et al. 2019). Similar to the 2011 case, SESR was correlated to the drought identified by the USDM, with that correlation generally being statistically significant. But it underestimated where the drought was most intense (Fig. 6). In particular, it tended to underestimate persistence of the drought slightly or failed to identify drought altogether (Fig. 7). This is more prominent west of the Rocky Mountains. But the monthly average (Fig. 8) tends to agree well with the drought coverage for 2012 (Supplementary Figure 2). Therefore, SESR had

more trouble capturing the persistence of the drought, rather than the spatial coverage east of the Rocky Mountains. In addition, SESR underestimated the severity of the drought in most locations, particularly where the drought was most severe, as well as Georgia, where the difference was statistically significant.

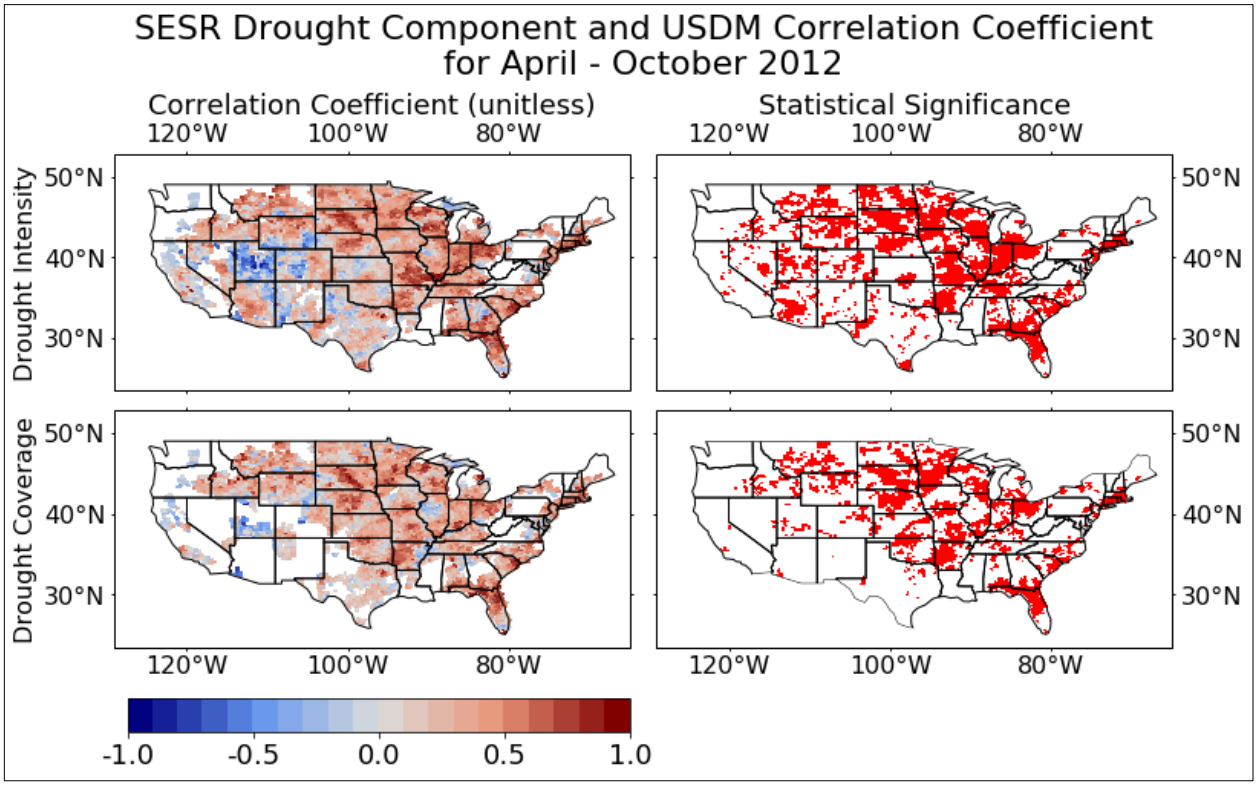

Figure 6. Correlation coefficient of the SESR drought component with the USDM for the growing season of 2012. (left) Correlation coefficient between the SESR drought component and USDM, and (right) the 95% statistical significance, calculated using the Monte-Carlo method with N = 5000. Statistical comparisons are for (top) drought coverage and intensity and (bottom) only drought coverage.

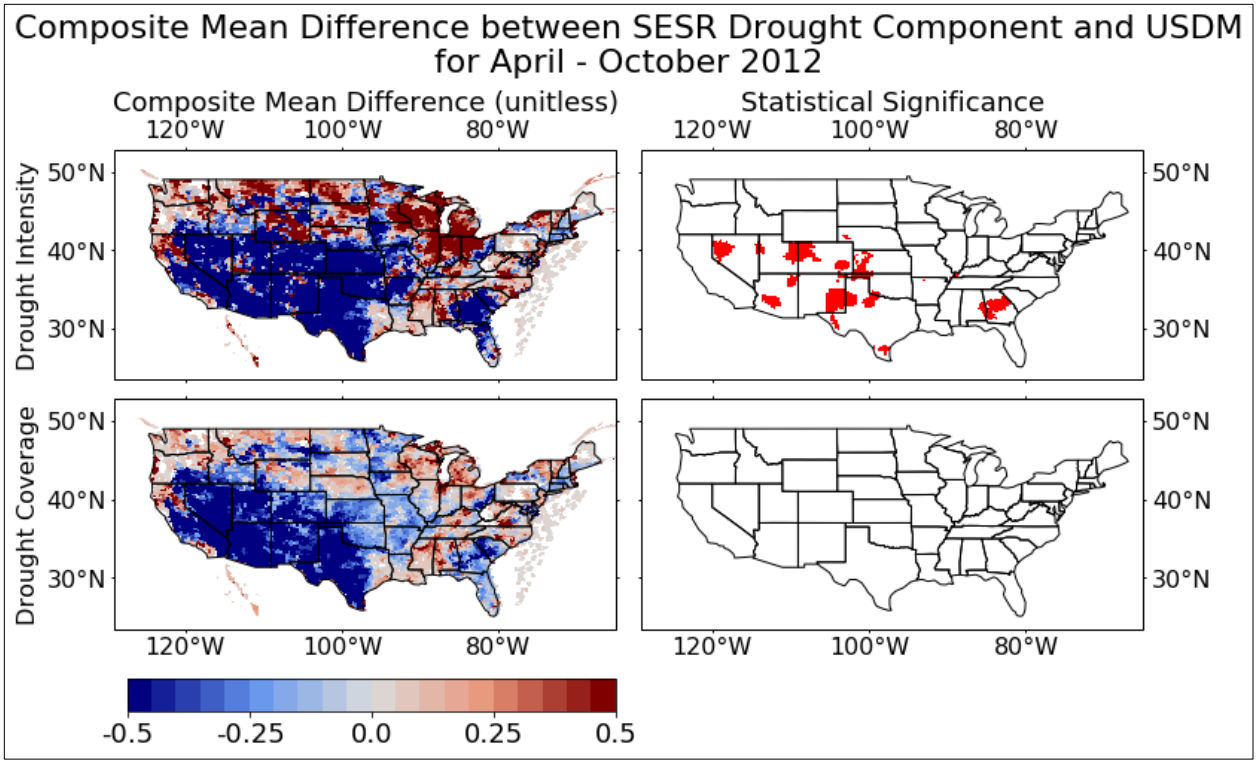

Figure 7. Composite mean difference between the SESR drought component and the USDM for the growing season of 2012. (left) Composite mean difference between the SESR drought component and the USDM, and (right) the 95% statistical significance, calculated using the Monte-Carlo method with N = 5000. Statistical comparisons are for (top) drought coverage and intensity and (bottom) only drought coverage.

Examining Figure 8, little drought was identified during May, save along the upper Mississippi delta, following the above normal precipitation at the start of the growing season (Basara et al. 2019). However, as time proceeded, under above normal temperature and a lack of precipitation, the drought worsened and propagated eastward into the upper Mississippi River region and lower Ohio River Valley in June, intensified in these regions, and propagated into western Iowa and the Corn Belt region during July and August. Again, SESR tended to identify D2 and occasionally

D3 drought with some D4 drought in Indiana and surrounding states, whereas the USDM identified widespread D3 and D4 drought for this event. In addition, SESR propagated the drought northwest into the Dakotas much faster than the USDM did. Hence, it seems SESR does not identify the most severe cases on its own. However, it does capture the spatial extend and regions of significant drought effectively.

With respect to rapid intensification during 2012, it began in May in central Kansas and northern Missouri and steadily spread into Nebraska in June, and to the rest of the Corn Belt in July (Fig. 8). These results are in general agreement with Basara et al. (2019); McEvoy et al. (2016); Otkin et al. (2014). More specifically, the algorithm managed to yield individual regions that experienced rapid intensification found in Basara et al. (2019), such as north central Kansas in May, north central Oklahoma in June, north central Missouri in May, central Nebraska in June, and southeast Minnesota in August, as seen in Supplementary Figure 3. Additionally, the flash component identified rapid intensification in some regions not previously discussed in connection with the 2012 drought such as southern Texas, and isolated parts of the Deep South. It is possible these are rapid intensification events were not connected with the drought.

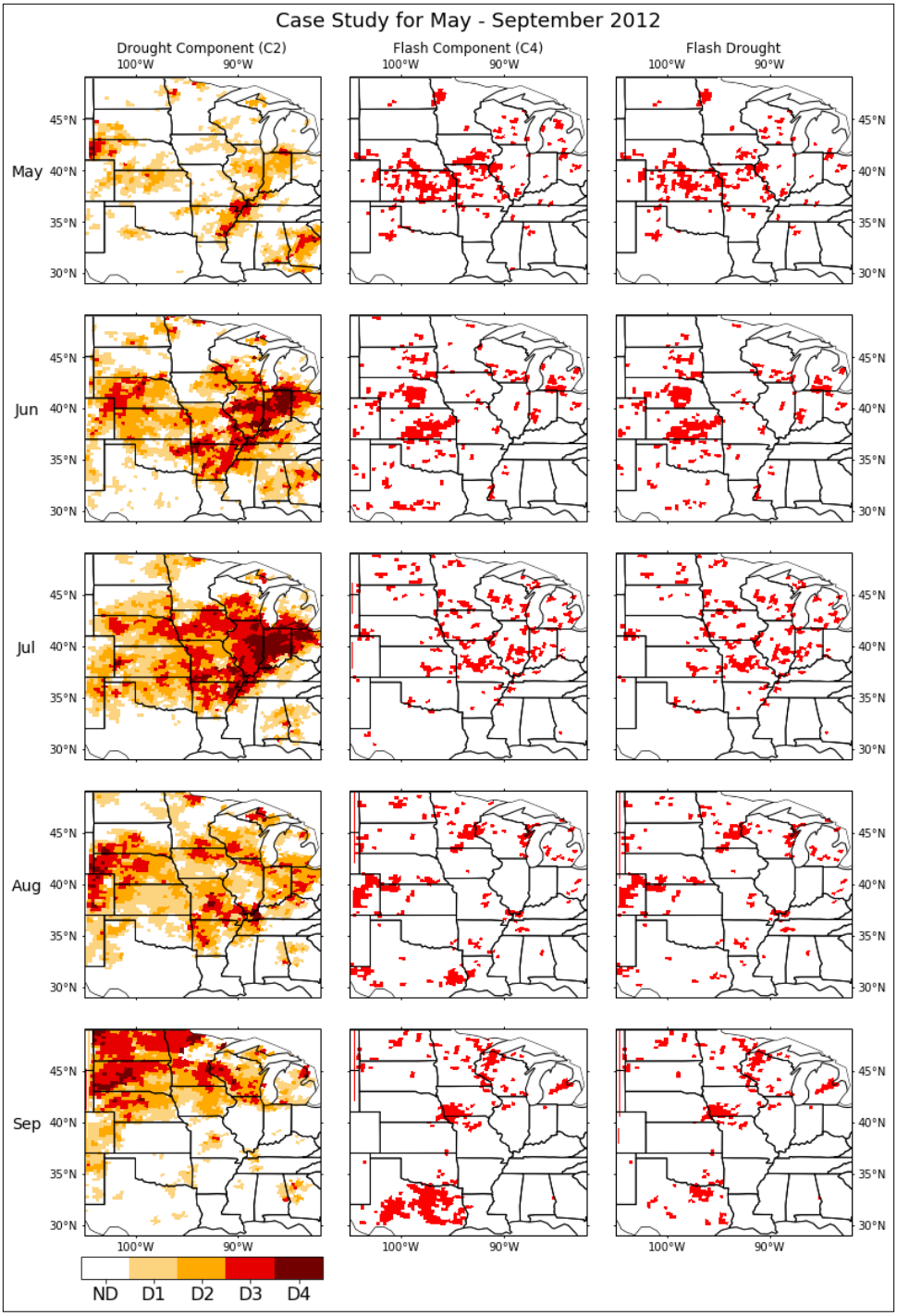

Figure 8. Case study for the growing season of 2012 (excluding March, April, and October). (left) Monthly average drought component (coverage and intensity), (center) monthly coverage of the SESR flash component, and (right) monthly coverage of flash drought. Red color indicates SESR flash component/drought was newly identified for at least 1 pentad in that month.

c. 2019: Weak Drought

Above normal precipitation occurred east of the Rocky Mountains throughout the months of May, June, and part of July during 2019. However, precipitation subsequently decreased significantly causing many areas to experience rapid drying. However, few regions reached drought conditions due to the preceding excessive precipitation, and as such 2019 represents an opportunity to examine and test how SESR performs with weak to non drought conditions even though rapid drying occurred. Specifically, drought identification showed notable improvements from the extreme cases, with SESR being more strongly, and statistically significantly, correlated to the USDM where drought occurred (Fig. 9). In addition, SESR continued to underestimate the persistence or coverage and intensity of drought in Texas, though the degree of underestimation was less than in 2011 or 2012 (Fig. 10). Figure 11 yielded little to no drought present during May, which continued into June and July, indicating that SESR reacted well with above normal precipitation events. In addition, SESR captured drought that did occur in the Pacific Northwest. In general, SESR did not show drought developing until August and September, and this mostly in the southwestern part of the U.S.

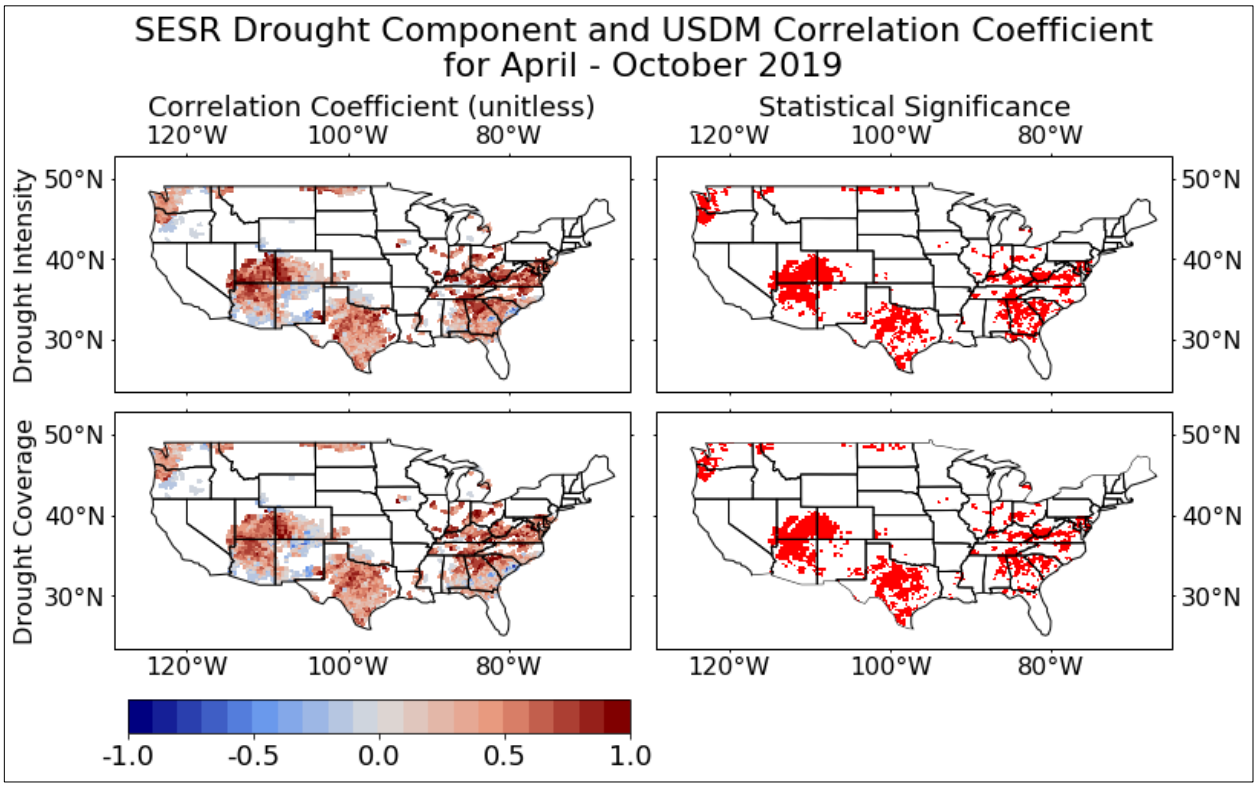

Figure 9. Correlation coefficient of the SESR drought component with the USDM for the growing season of 2019. (left) Correlation coefficient between the SESR drought component and USDM, and (right) the 95% statistical significance, calculated using the Monte-Carlo method with N = 5000. Statistical comparisons are for (top) drought coverage and intensity and (bottom) only drought coverage.

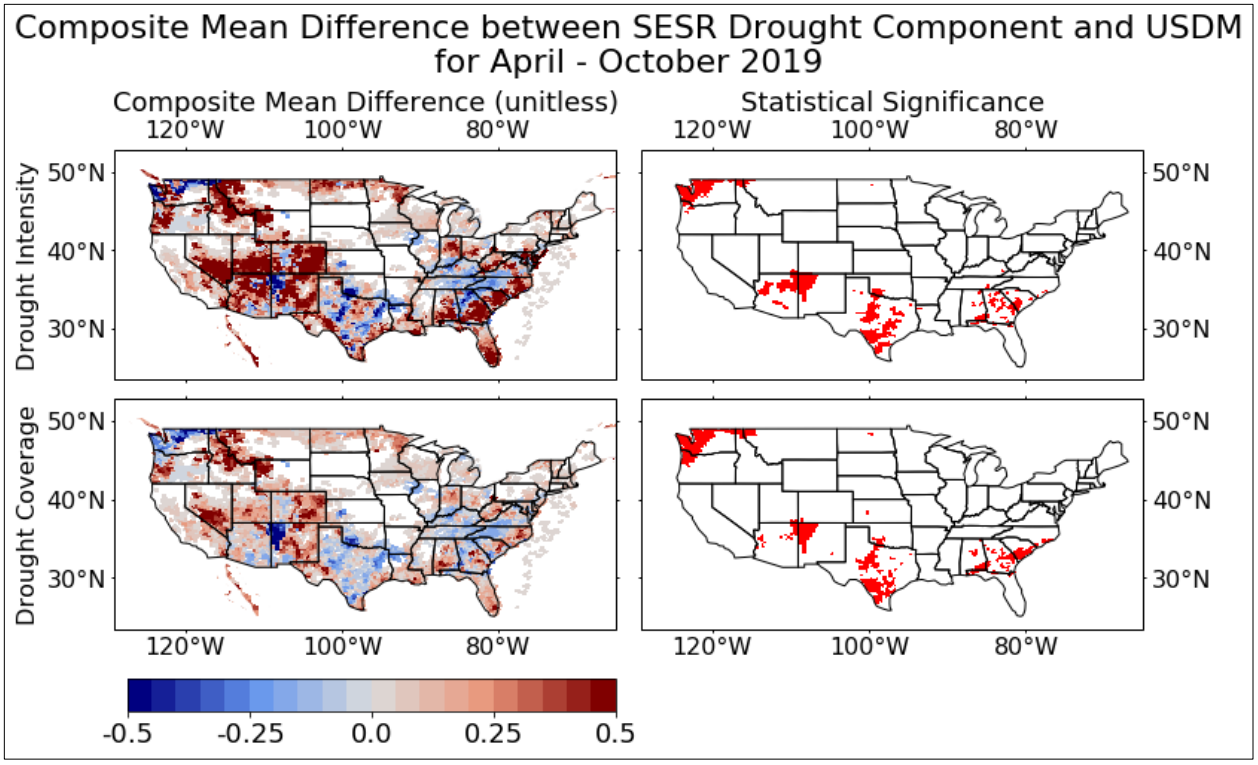

Figure 10. Composite mean difference between the SESR drought component and the USDM for the growing season of 2019. (left) Composite mean difference between the SESR drought component and the USDM, and (right) the 95% statistical significance, calculated using the Monte-Carlo method with N = 5000. Statistical comparisons are for (top) drought coverage and intensity and (bottom) only drought coverage.

The flash component representing rapid intensification was identified in numerous locations, most of which were west of the Rocky Mountains. It starts with rapid intensification identified in the lower Colorado River in May and expanded into the Mojave and southern Nevada in June, into Central Valley and Utah in July (Fig. 11). However, little to no flash drought was identified, excepting parts of the Coastal Plains, as few regions reached drought status and few occurred where the rapid intensification occurred.

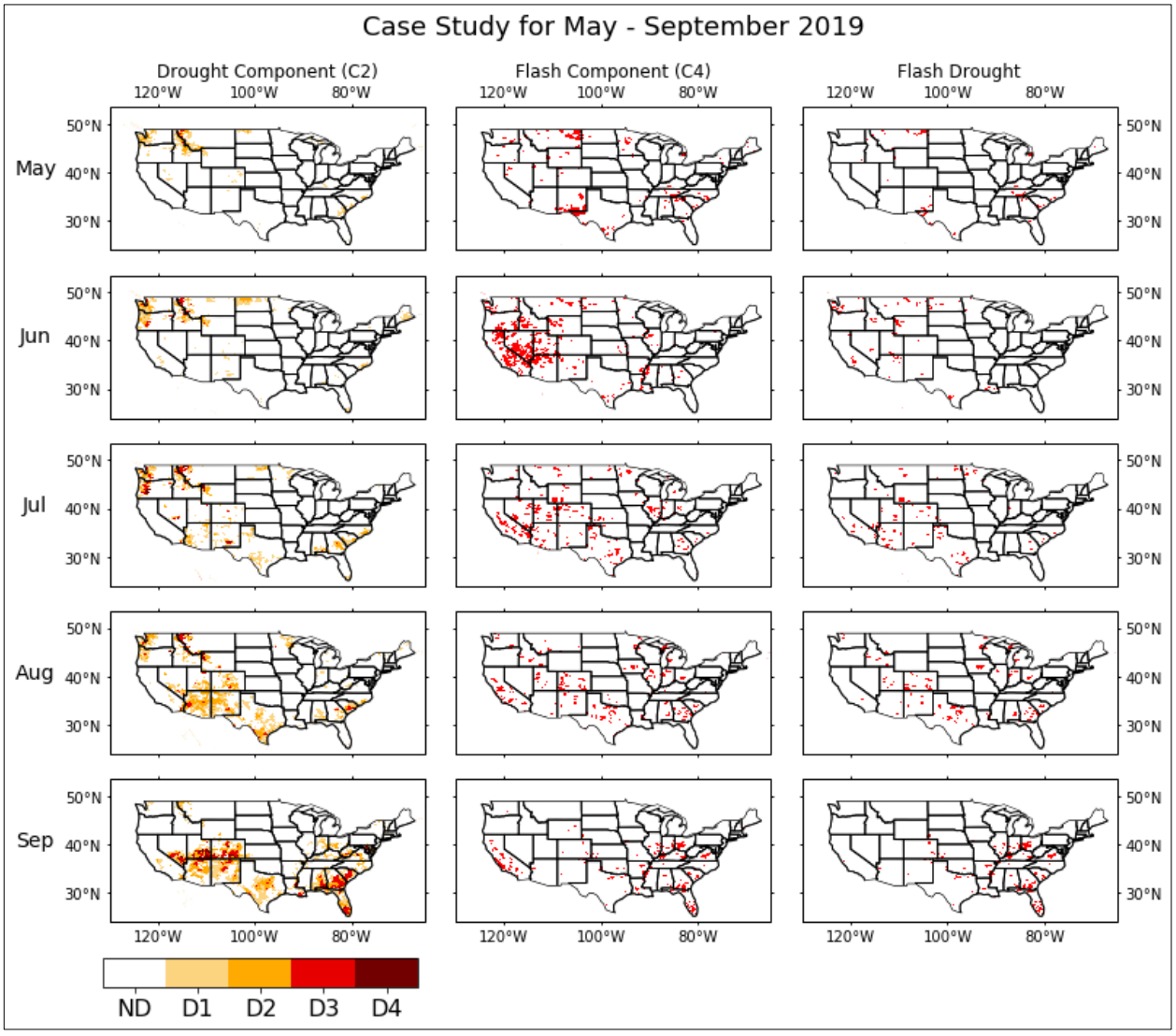

Figure 11. Case study for the growing season of 2019 (excluding March, April, and October). (left) Monthly average drought component (coverage and intensity), (center) monthly coverage of the SESR flash component, and (right) monthly coverage of flash drought. Red color indicates SESR flash component/drought was newly identified for at least 1 pentad in that month.

d. 1988: Northern United States and Great Lakes

The great drought of 1988 is a well-studied case in which severe drought occurred in the northern and central U.S. (e.g. Kim and Rhee 2016; Kim et al. 2019). The results produced by SESR during 1988 identified drought conditions in the Northern Plains and Great Lakes region in May, which quickly intensified during June (Fig. 12). SESR identified mostly D4 drought for this event. Furthermore, the rapid spread and intensification of drought from May to July saw wide spread rapid intensification throughout many parts of the northern U.S. via the flash component, from Montana to Indiana and as far south as Texas. Most of these areas also fell into flash drought with an exception being around the Ozark Mountains.

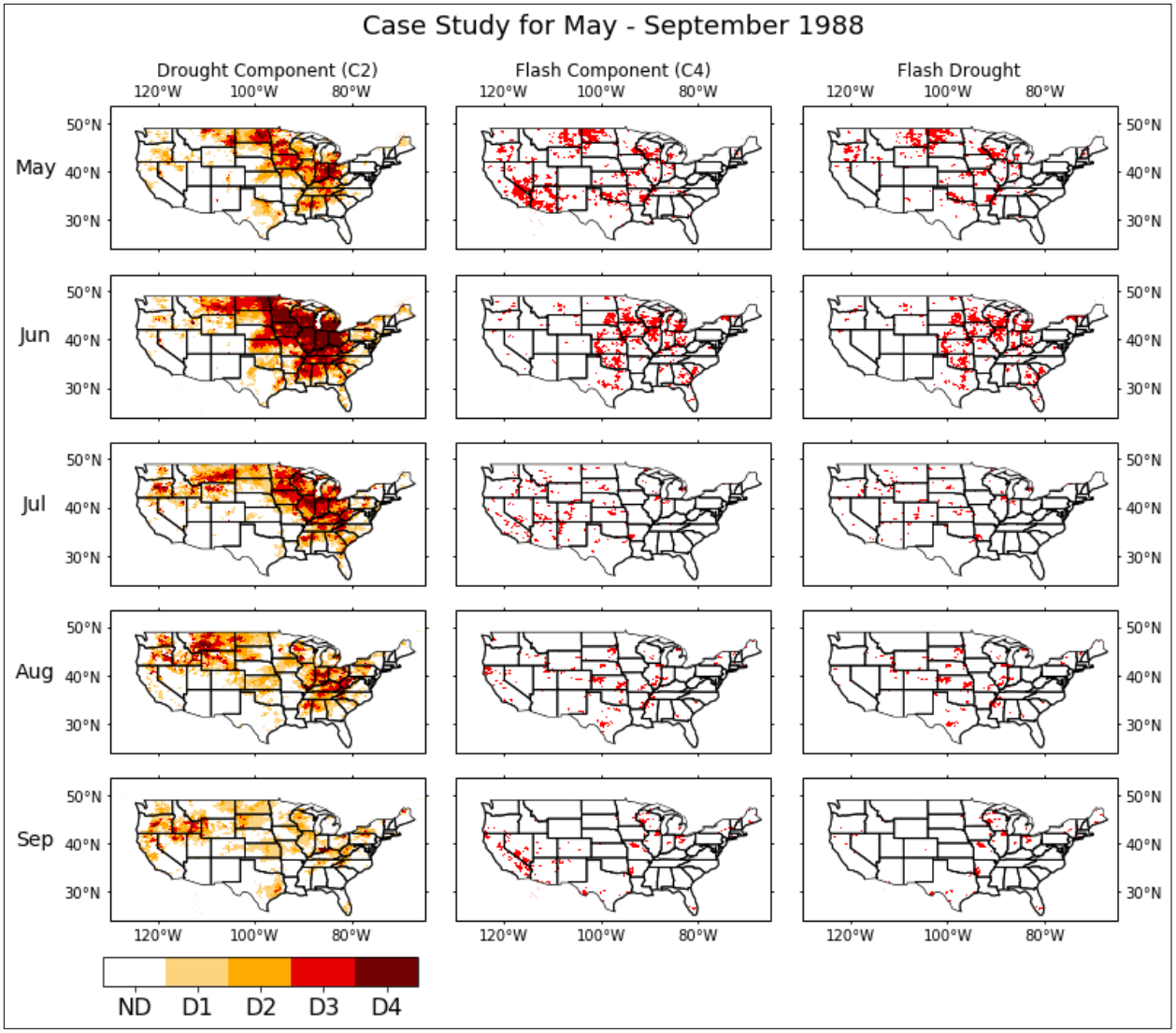

Figure 12. Case study for the growing season of 1988 (excluding March, April, and October). (left) Monthly average drought component (coverage and intensity), (center) monthly coverage of the SESR flash component, and (right) monthly coverage of flash drought. Red color indicates SESR flash component/drought was newly identified for at least 1 pentad in that month.

e. 2003: Midwestern United States

Finally, drought developed rapidly during the summer months across the Midwestern U.S., particularly around Iowa, Nebraska, Illinois, and Wisconsin during 2003 (Otkin et al. 2014). Based on SESR (Fig. 13), this event began with drought present in northern Illinois and Missouri during May. This drought weakened in June due to precipitation events which moderated environmental conditions. However, by July, drought had started to redevelop in many parts of the central and southern Great Plains, and subsequently propagated northward into Iowa and the Corn Belt region where it rapidly intensified into a significant drought event. This was mirrored in the flash component, which showed rapid drying originally in July in the central and southern Great Plains, which quickly spread into Nebraska, Iowa, and the rest of the Corn Belt by the end of August. These results are in close agreement with the spatial coverage and timing of the flash drought found in Otkin et al. (2014), which can be seen in Supplementary Figure 4.

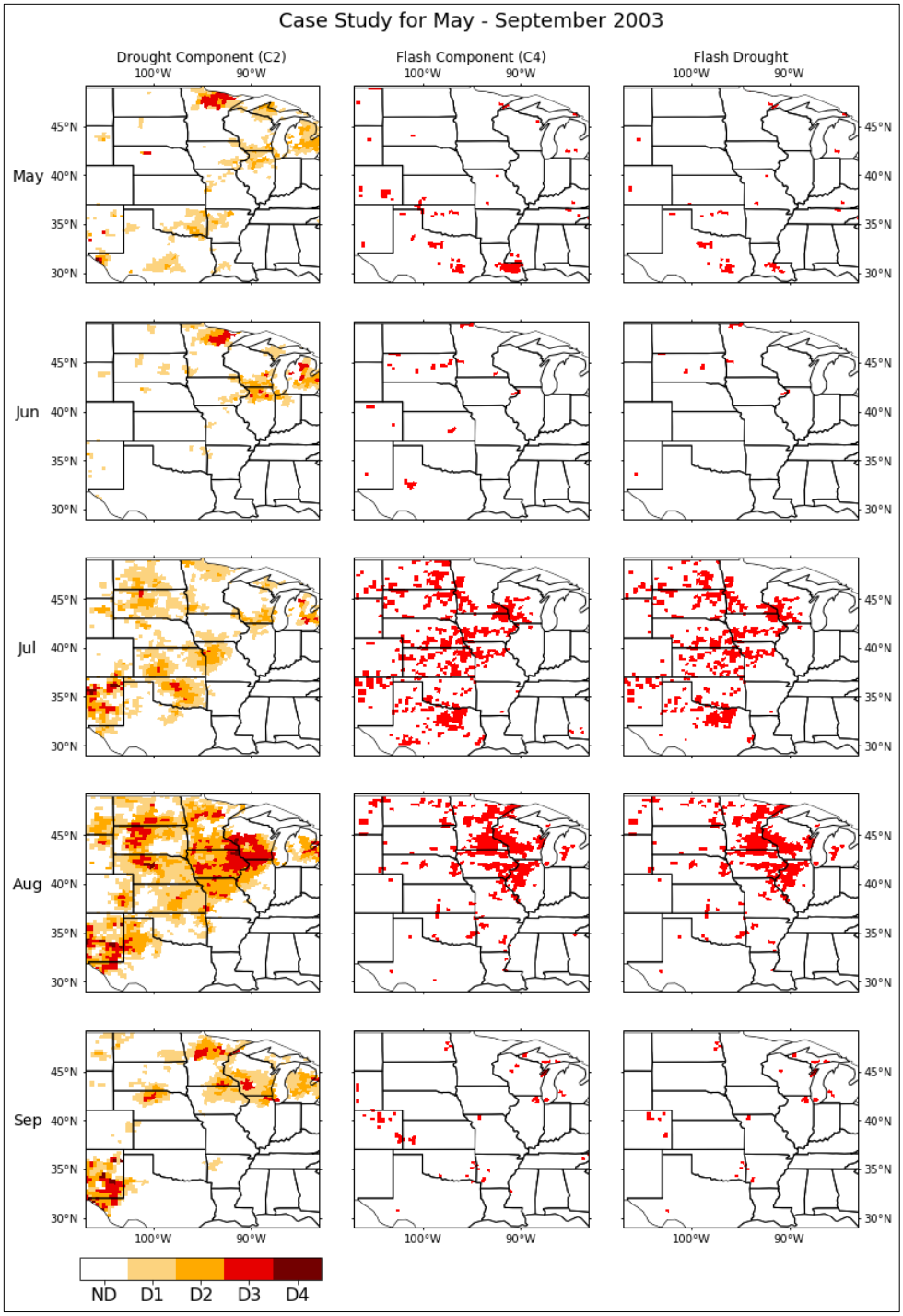

Figure 13. Case study for the growing season of 2003 (excluding March, April, and October). (left) Monthly average drought component (coverage and intensity), (center) monthly coverage of the SESR flash component, and (right) monthly coverage of flash drought. Red color indicates SESR flash component/drought was newly identified for at least 1 pentad in that month.

4. Climatology

a. SESR Drought Component

The first component of the climatological analysis focused on the overall performance of the SESR drought component. The results of the comparisons between the USDM and drought component for all years (2010 – 2019) is shown in Figure 14 and demonstrates the datasets were well correlated during the period. In particular, the USDM and SESR have a high correlation, across the Pacific Northwest, Deep South, and Great Lakes region, with the correlation being statistically significant in those places further regions where SESR is particularly good at identifying drought. In addition, the correlation did not change appreciably between the correlation for drought coverage (bottom left panel) and for drought coverage and intensity (top left panel). That is, on a climatological average, SESR was able to identify not only where drought was present (bottom panels), but also which regions experienced more severe drought (top panels), which one might expect based on the results of Kim and Rhee (2016) and Kim et al. (2019). The correlation does tend to decreases to near 0 in numerous locations in the Intermountain West. In addition, the small correlation holds for the Ohio River Valley, particularly where the topography of the Appalachian Mountains is most complex. Across the West, the composite mean difference between the USDM and drought component (Fig. 15) illustrates that SESR has difficulty identifying drought within the region, often failing to identify drought when one occurs (bottom panels). Further when it does identify drought in the Intermountain West, it tends to underestimate the intensity of the drought (hence the stronger mean difference in the top panels). Conversely, in the Ohio River Valley SESR tends to overestimate the intensity of drought. In contrast to this, the composite difference is small and

near zero (no difference, SESR identifies drought well) in the Northern and Central Great Plains, Pacific Northwest, as well as parts of the Deep South.

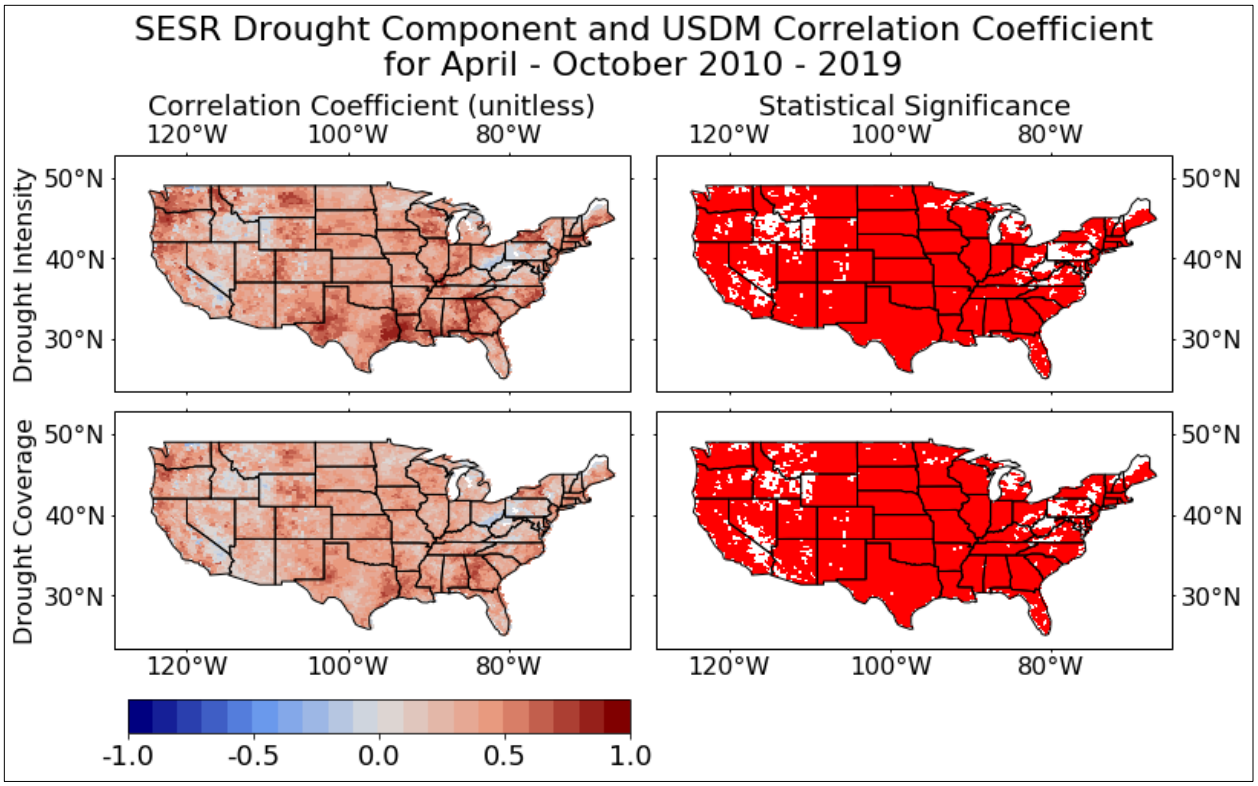

Figure 14. Correlation coefficient (left) for the SESR drought component and USDM and statistical significance (right) for the corresponding correlation coefficients for coverage and intensity (top) and just drought coverage (bottom) for growing season of 2010 – 2019.

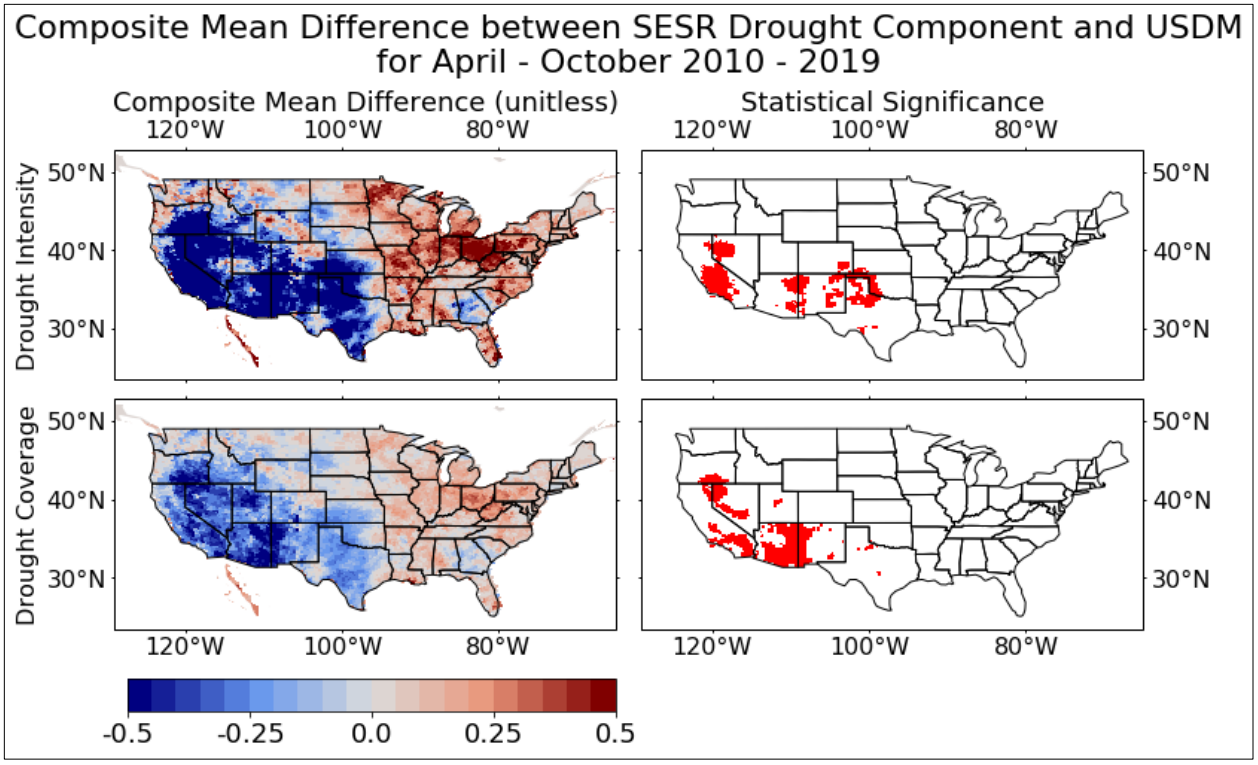

Figure 15. Composite mean difference (left) between the SESR drought component and USDM and statistical significance (right) for the corresponding composite difference for coverage and intensity (top) and just drought coverage (bottom) for growing season of 2010 – 2019.

To quantify the spatial coherency of drought identification between SESR and the USDM for each pentad and grid point, those locales where agreement occurred (the binary values were the same) were given a value of 1, and conversely those locales where disagreement occurred were given a value of 0. As such, the computed mean in time (which, under this binary classification, is the sum of all pentads with agreement divided by the total number of pentads) displays the frequency of correct drought identification by SESR when compared to the USDM (Fig. 16; left panel). A critical result of the analysis is the notable agreement between the USDM and SESR that consistently occurred across the majority of the U.S., particularly east of the Mississippi

River and Pacific Northwest. Further, weaker to neutral agreement occurred in the semi-arid Great Plains (namely the Southern Great Plains), portions of Georgia, and the Intermountain West with frequent disagreement in the arid Desert Southwest.

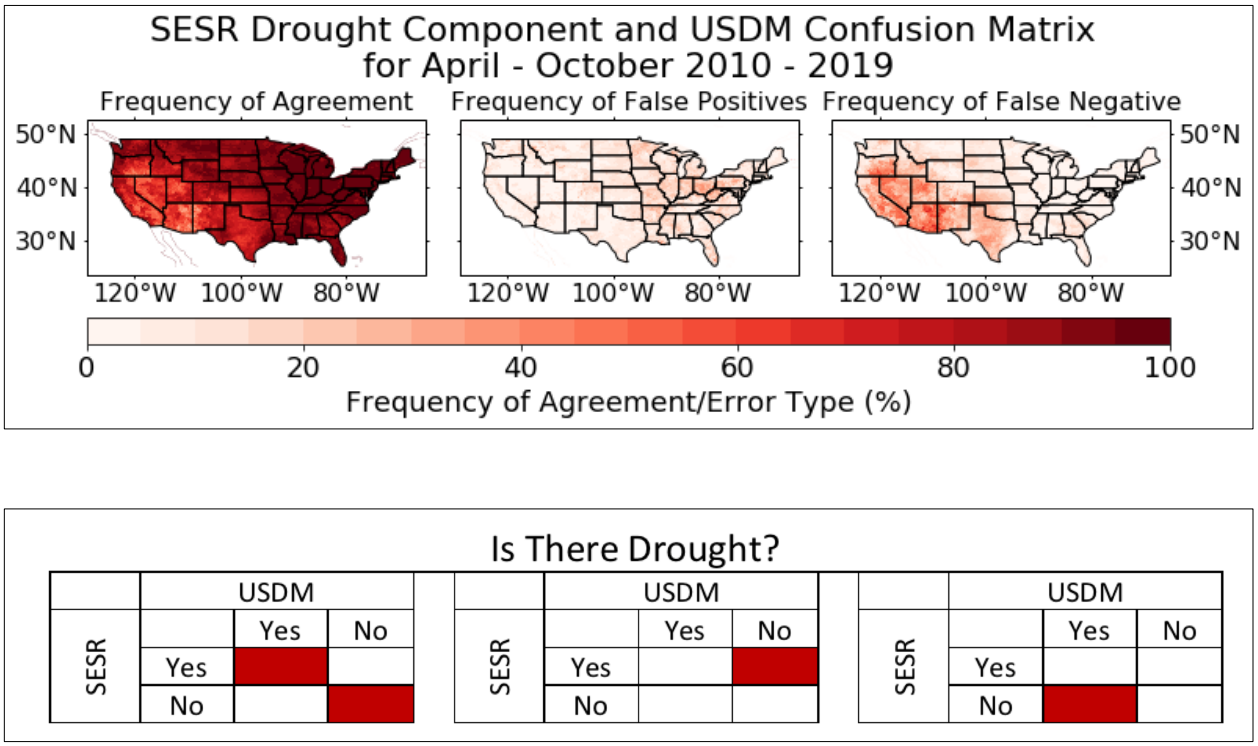

Figure 16. Spatial distribution of averaged agreement of drought (SESR drought component and USDM both identified or did not identify drought at the same time; left), false positive error (center), and false negative error (right). Where the USDM and SESR drought component agreed (both have true or false for drought identified), a value of 1 is given, and 0 otherwise. The mean then gives the frequency of correct drought identification (left). Where the USDM has no drought and the SESR drought component has drought, a value of 1 is given and 0 otherwise. The average gives the frequency of false positive type errors (center). If the USDM has drought, and the SESR drought component has no drought, a value of 1 is given, and 0 otherwise. The

average gives the frequency of false negative type errors (right). The confusion matrix below shows the type of error to the corresponding map.

To determine the type of error a value of 1 was assigned when SESR identified drought but the USDM did not and 0 otherwise (center panel). Conversely, when the USDM identified drought but SESR did not, a value of 1 was given and 0 otherwise (right panel). Thus, the mean in time in the center and right panels of Figure 16 provides the frequency of false positive and false negative errors respectively. When compared with the results of the composite mean difference (Fig. 15), SESR more frequently arrived at a false negative (or a "miss") whereby it failed to identify drought when needed in the semi-arid to arid regions and portions Georgia. This could explain the reduced correlation found in the Southern Great Plains and around the more arid regions. However, more false positives (or "false alarms") were identified by SESR east of the Mississippi River centered around the Great Lakes region and the Ohio River Valley. An additional possibility is that SESR becomes a good indicator of drought in regions where there is moderate to high transpiration from the vegetation, so that the ET and PET become an accurate measure of vegetative stress. This would also explain the low correlation in the Intermountain West and Southern Plains, where the vegetation retains moisture in the arid environments, but works well in the Northern Plains and Pacific Northwest, where the agricultural crops and temperate vegetation transpire at a moderate rate. However, this does not explain the poor performance in Georgia and Ohio River Valley, and more work needs to be done to determine the reason for this.

b. SESR Flash Component

To refine the analysis further, the climatologies of flash drought and the flash component were completed and displayed in Figure 17. Given the flash drought climatology was based on the method of Christian et al. (2019), the analysis was consistent in identifying hotspots in the Great Plains, the Yazoo Delta, the Coastal Plains, and various areas along the East Coast. In general, the hotspots are located around various precipitation gradients and/or agricultural regions, in general agreement with previous studies (Chen et al. 2019; Christian et al. 2019). The flash component analysis displays similar hotspots with an increased annual frequency of about 10% - 20%. However, an additional expansive hotspot in the flash component was located across the Desert Southwest, and into central Nevada. Further, other areas in the Intermountain West, including Central Valley and Great Salt Lake and surrounding areas yielded a higher frequency of rapid intensification not highlighted in the flash drought climatology. Overall, regions of rapid intensification occurred more frequently than flash drought as expected given rapid intensification is only one component of flash drought development. However, east of the Rocky Mountains rapid intensification (i.e., the flash component) is more closely linked to flash drought development while west of the Rocky Mountains there are frequent rapid intensification events (more frequently than east of the Rocky Mountains) but with few events reaching drought status and achieving flash drought development.

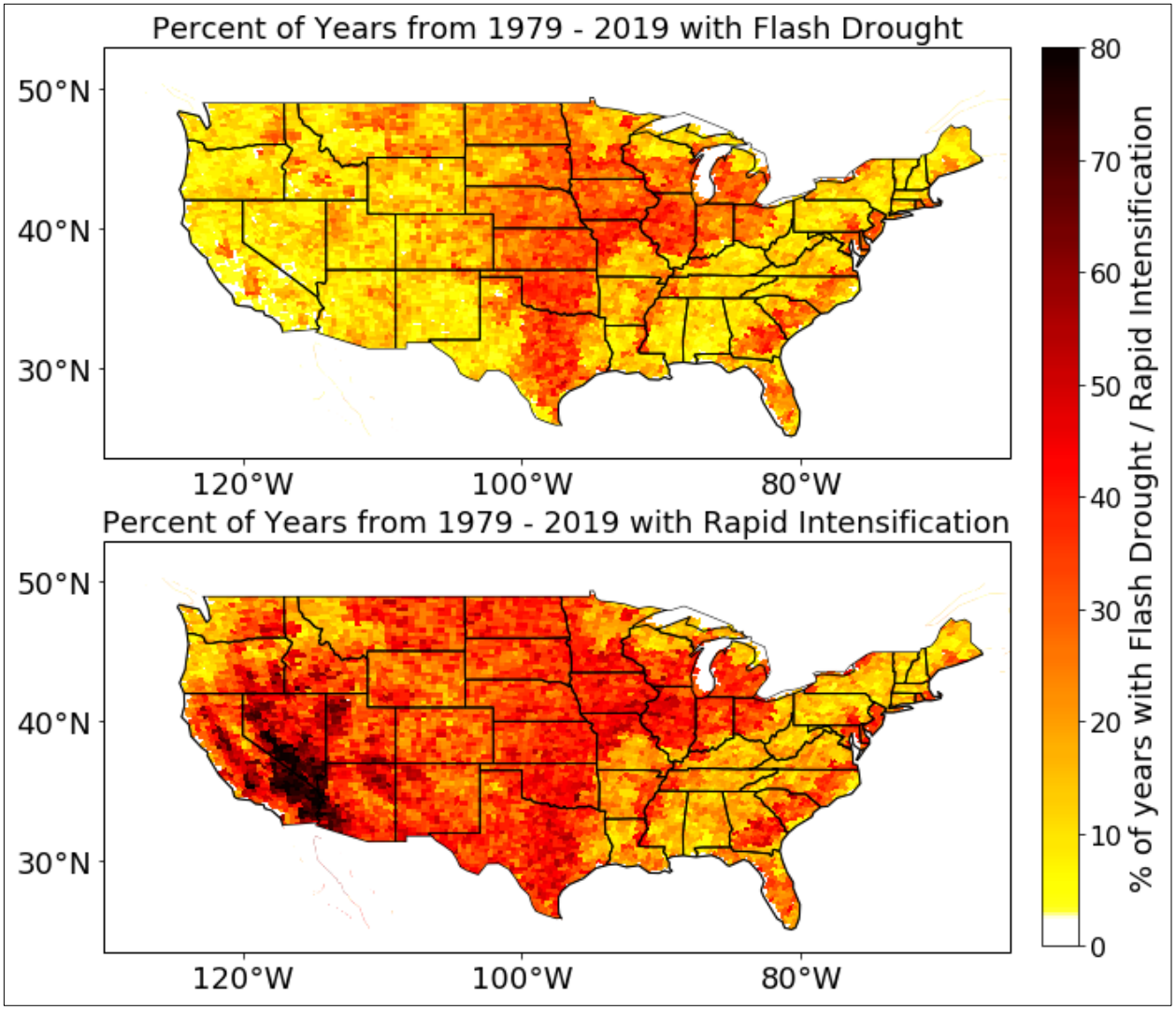

Figure 17. Climatological average (from 1979 – 2019) of flash drought (top) and the flash component (bottom).

To examine areas with rapid intensification (flash component) but no, drought, the correlation coefficient and composite mean difference were computed between the two variables and plotted in Figure 18. The correlation coefficient was large with values between 0.5 and 1 in most locations east of the Rockies. However, the correlation values drop quickly and vary from 0 to

0.25 west of the Rocky Mountains. This result is also displayed in Figure 19, where the difference in areal coverage for rapid intensification and flash drought decreases when only the area east of the Rocky Mountains is considered (i.e., east of 105˚W). Figure 19 displays that for locations east of the Rockies, the temporal peak in flash drought and rapid intensification (flash component) events occurs within July and August which agrees with the seasonality of flash drought noted by Chen et al. (2019), Christian et al. (2019), and Noguera et al. (2020). Finally, the composite difference for the flash component yielded near zero values (no difference) east of the Rockies with the greatest differences across the Intermountain West and the Mojave Desert. This agrees with the previous results that the flash component plays the prominent role in flash drought development east of the Rockies, whereas the drought component plays a more prominent role west of the Rockies.

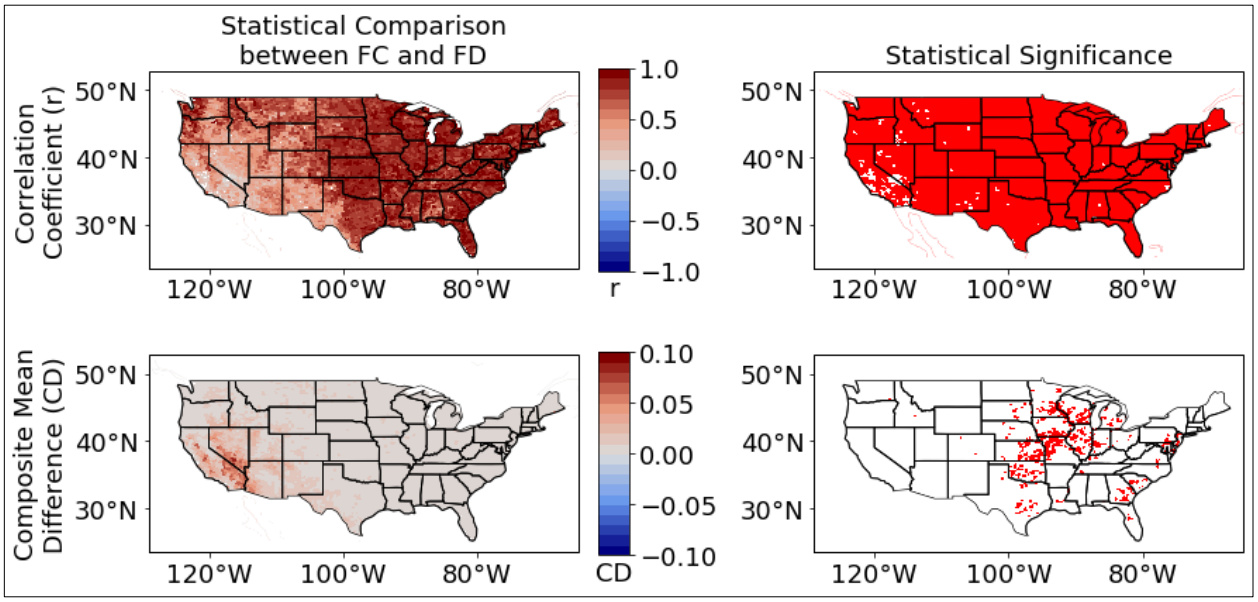

Figure 18. Correlation coefficient between the SESR flash component and flash drought (top) and the composite mean difference between the flash component and flash drought (bottom) for all years (1979 – 2019; left) and statistical significance at the 95% level for the corresponding

statistical comparison (left). Statistical significance was calculated via the Monte-Carlo method with N = 5000.

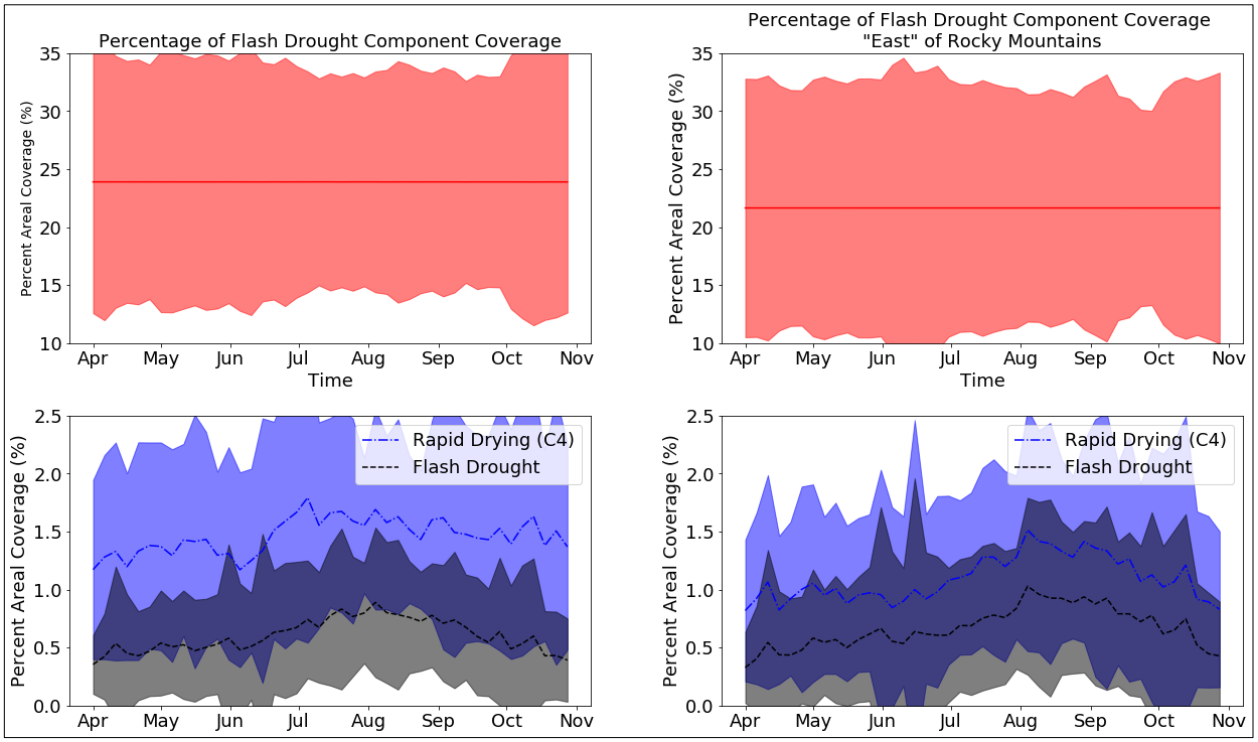

Figure 19. The annual average percentage of areal coverage for drought (top, red line), rapid intensification (bottom panel, blue line), and flash drought (bottom panel, black line) spanning 1979 – 2019 in time for the whole domain (U.S.; left) and across the domain east of -105˚E to exclude the Intermountain West (right). Shaded areas denote 1 standard deviation variability.

5. Discussion and Conclusions

This study utilized the method of flash drought identification developed by Christian et al. (2019) and separated flash drought in the (1) drought and (2) flash components. These components were examined separately to investigate the evolution of drought and rapid intensification (used synonymously with the flash component) and to verify the accuracy of these components for several different cases. The verification of the drought component was completed by comparing the SESR results to the USDM from 2010 to 2019, and the flash component was compared to the results of previous studies. For the case studies, two extreme years previously studied frequently (2011 and 2012), a year with little to no drought (2019), and two years with extreme drought that did not have a quantitative comparison (1988 and 2003) were chosen. In addition, and the drought component was evaluated over all years (2019 – 2019) in the USDM dataset to examine how well SESR identified drought. The flash component was evaluated over all years (1979 – 2019) in the NARR dataset to determine the climatological characteristics of rapid intensification.

Overall, SESR has the potential to identify drought as a solo metric. It successfully mapped the spatial extent of drought events and identified areas where the drought is strongest. For example, SESR was able to almost perfectly recreate the spatial extend of the 2011 drought found in Vicente-Serrano et al. (2018) and Kim et al. (2019). However, SESR has deficiencies with extreme events, often underestimating how intense the drought is and how persistent it is (that is, SESR may be sensitive to moderating events and fail to identify drought on short time scales when its impacts are still present). One reason for this is the use of percentiles to classify

drought. For example, SESR identified mostly D4 drought for the 1988 drought. It is possible that, due to the use of percentiles for drought classification, this year resulted in some of the underestimations of drought in other years. That is, D4 drought is identified for percentiles below 2%, and for a 41 year dataset that means each grid point only gets 1 year (2 years with the offset) in which to identify D4 drought. Given that this occurred in 1988, it is possible that some regions that experienced severe drought later (e.g. 2012), the percentiles were above the 2% mark because of this.

However, on a climatological scale, SESR continued to demonstrated strong potential in being able to identify drought conditions including and beyond flash drought. However, SESR as a stand-alone drought metric yielded deficiencies across arid and semi-arid regions and in regions of complex topography. In the case of the latter, given the challenges in parameterizing the state of the terrestrial surface in areas of complex terrain, there is uncertainty as to whether the deficiencies are due to the SESR method or the reanalysis. Given that errors in SESR identified drought can be generally separated spatially by arid to non-arid regions, it is possible that the addition of precipitation information (such as SPI) may a critical addition in correctly identifying drought.

Overall, the SESR performed well in identifying drought in the Pacific Northwest, the Northern and Central Plains, the majority of the Deep South, the Great Lakes Regions, and the Northeast. It had trouble identifying drought in the Intermountain West, Georgia, and the Ohio River

Valley, and it had some difficulty in the Southern Plains. A possible explanation is that aridity and, to a lesser degree, temperature governs how well SESR did. That is, its best performance was in more humid regions, whereas it struggled in more arid regions. Though this does not explain everything (e.g., the good performance in the more arid Northern Plains and poor performance in Georgia), it tends to match general observations that the performance of SESR can generally be separated by aridity. Another possibility is that SESR performs well in regions that experience moderate to high transpiration from the vegetation. This is because ET is using transpiration to measure vegetation health and stress. If the vegetation conserves moisture, as conifers and most arid vegetation do, then ET may not be a good measure for vegetation health. This would explain the good performance in the Pacific Northwest, despite the importance of wintertime precipitation (which was excluded for this study), as it has more temperate vegetation that transpires more readily. It would also explain the good performance in the Northern Plains, which is more agricultural based than the western part of the Southern Plains, which has more moisture conservative vegetation. That is, regions that are more moisture stressed in the Southern Plains are used more for ranching, and they thus contain vegetation that is more likely to conserve moisture. However, the transpiration of vegetation does not explain the poor performance in Georgia. Lastly, the poor performance in the Intermountain West could also be related to its hydrologic processes in that region. That is, the main precipitation in the Intermountain West is in snowpack during the winter, which was excluded in this study. SESR might, therefore, be a poor indicator of the hydrologic processes that occur in that region of the country (i.e., SESR is not a one size fits all index for drought). It is suggested then that more work be done to investigate the reasons for why SESR succeeds and fails where it does. In

particular, it is suggested to focus on Georgia, as the reason for SESR's poor performance there is unknown.

In addition, the difficulty SESR showed in representing droughts, particularly in arid regions and in extreme scenarios, and the fact that the percentiles can only identify D4 drought in one year out the dataset, suggests that it does need help from another index, variable, or dataset to help accurately represent drought. Because ET incorporates soil moisture, vegetation conditions, and general moisture conditions (Chen et al. 1996), and PET incorporates temperature and soil fluxes (Mahrt and Ek 1984), the variable most indirectly represented by SESR is precipitation. Thus, a precipitation index such as SPI would be recommended to help identify drought. A caveat that should be noted, however, is that there is some level of subjectivity the USDM (Leasor et al. 2020) and the USDM uses multiple indices across multiple temporal scales to identify drought (McEvoy et al. 2016), and this should be kept in mind when comparing it to a single variable at a single time scale. In fact, SESR does an excellent job at drought identification in this sense.

The flash component proved difficult to verify as no other method of quantifying rapid intensification is available for comparison. When compared to the results of individual flash drought events, SESR performed well and was able to identify rapid intensification, successfully capturing the onset of flash drought described by Otkin et al. (2013) and McEvoy et al. (2016) in 2011 and Basara et al. (2019) in 2012. On a climate scale, the flash component showed a similar climatology to flash drought east of the Rocky Mountains. West of the Rocky Mountains, it

yielded a large frequency of rapid intensification events. East of the Rocky Mountains, rapid intensification or the flash component plays a critical role in flash drought occurrence, agreeing with previous studies (Liu et al. 2020; Noguera et al. 2020). Further in this region, while rapid intensification without drought events do occur, they are limited and uncommon. However, west of the Rocky Mountains, the situation reverses with frequent rapid intensification events but very few flash droughts events. This suggests that the critical factor in this region is the drought component. There may be several reasons for this dichotomy. For example, in the west the rapid intensification events may be due to the climatological onset or termination of the seasonal monsoon conditions in that region. As such, precipitation is often followed by rapid drying due to the arid nature of the region, but it would not necessarily enter drought (in Fig. 19, the peak in rapid intensification occurs in July when the Intermountain West is included which is shortly after or during monsoon season whereas the peak occurs in August and September east of the Rockies). It also feasible that SESR may be ill defined in the Intermountain West due to the inherent arid nature of the region, emphasis on ET, and the role of winter precipitation instead of summer precipitation (Otkin et al. 2014) at higher elevations, which could lead to the frequent misses in drought identification. Finally, it is also possible this might be a reanalysis and resolution issue due to the complex topography of the region. Overall, there are several potential reasons why a high frequency rapid intensification events west of the Rockies occurs with limited drought and more investigation needs to be completed to determine the physical mechanisms.

In conclusion, this study successfully separated the components of flash drought into rapid intensification and drought components. It was determined that rapid intensification plays a

prominent role in flash drought development east of the Rocky Mountains. Therefore, attempts to identify flash drought in real time, or predict them must be able to capture that. Because this is connected with land-atmosphere exchanges (Kim and Rhee 2016; Chen et al. 2019; Christian et al. 2019; Wakefield et al. 2019), these exchanges need to be accurately modelled to predict flash drought events. Additionally, because this method can be used with any gridded dataset, it can be used to help identify flash droughts in real time or predict them, so long as the dataset is in real time or predictive. However, it is also recommended to investigate how the results of this method changes with different climatological periods (e.g., use 10, 20, or 30 year averages instead of the 41 year average used in this study) to quantify how the these results may vary under a changing climate. In addition, SESR showed strong potential in being able to identify drought, though it had trouble in some locations such as the Intermountain West and Georgia. More investigation is recommended to determine why the performance was so low in Georgia, as the reason for SESR's poor performance there is unknown. It is also recommended to investigate SESR's ability to identify drought in union with a precipitation index, such as SPI, to determine how effectively precipitation can accommodate for SESR's deficiencies. Thus, overall, this analysis was able to separate flash drought into components and provide a means to quantify rapid intensification and drought using SESR, providing a new way to study flash drought events.

References

American Meteorological Society, A. M. S., 1997: Meteorological drought-policy statement. *Bulletin of the American Meteorological Society*, **78**, 847–849.

Basara, J. B., J. I. Christian, R. A. Wakefield, J. A. Otkin, E. H. Hunt, and D. P. Brown, 2019: The evolution, propagation, and spread of flash drought in the central United States during 2012. *Environmental Research Letters*, **14** (**8**), 084025, doi:10.1088/1748-9326/ab2cc0, URL http://dx.doi.org/10.1088/1748-9326/ab2cc0.

Chen, F., and Coauthors, 1996: Modeling of land surface evaporation by four schemes and comparison with fife observations. *Journal of Geophysical Research*, **101** (**D3**), 7251 – 7268.

Chen, L. G., J. Gottschalck, A. Hartman, D. Miskus, R. Tinker, and A. Artusa, 2019: Flash drought characteristics based on U.S. drought monitor. *Atmosphere*, **10** (**9**), 498, doi:10.3390/atmos10090498, URL http://dx.doi.org/10.3390/atmos10090498.

Christian, J. I., J. B. Basara, J. A. Otkin, E. D. Hunt, R. A. Wakefield, P. X. Flanagan, and X. Xiao, 2019: A methodology for flash drought identification: Application of flash drought frequency across the United States. *Journal of Hydrometeorology*, **20** (**5**), 833–846, doi:10.1175/jhm-d-18-0198.1, URL http://dx.doi.org/10.1175/JHM-D-18-0198.1.

Dai, A., 2011: Characteristics and trends in various forms of the palmer drought severity index during 1900–2008. *Journal of Geophysical Research*, **116** (**D12**), doi:10.1029/2010jd015541, URL http://dx.doi.org/10.1029/2010JD015541.

Ek, M. B., K. E. Mitchell, Y. Lin, E. Rogers, P. Grunmann, V. Koren, G. Gayno, and J. D. Tarpley, 2003: Implementation of Noah land surface model advances in the National Centers for Environmental Prediction operational mesoscale eta model. *Journal of Geophysical Research: Atmospheres*, **108** (**D22**), doi:10.1029/2002jd003296, URL http://dx.doi.org/ 10.1029/2002JD003296.

Flanagan, P. X., J. B. Basara, B. G. Illston, and J. A. Otkin, 2017: The effect of the dry line and convective initiation on drought evolution over Oklahoma during the 2011 drought. *Advances in Meteorology*, **2017**, 1–16, doi:10.1155/2017/8430743, URL http: //dx.doi.org/10.1155/2017/8430743.

Ford, T. W., D. B. McRoberts, S. M. Quiring, and R. E. Hall, 2015: On the utility of in situ soil moisture observations for flash drought early warning in Oklahoma, USA. *Geophysical Research Letters*, **42** (**22**), 9790–9798, doi:10.1002/2015gl066600, URL http://dx.doi.org/ 10.1002/2015GL066600.

Heim, R. R., 2002: A review of twentieth-century drought indices used in the United States. *Bulletin of the American Meteorological Society*, **83** (**8**), 1149–1166, doi:10.1175/ 1520-0477-83.8.1149, URL http://dx.doi.org/10.1175/1520-0477-83.8.1149.

Hobbins, M. T., A. Wood, D. J. McEvoy, J. L. Huntington, C. Morton, M. Anderson, and C. Hain, 2016: The evaporative demand drought index. Part I: Linking drought evolution to variations in evaporative demand. *Journal of Hydrometeorology*, **17** (**6**), 1745–1761, doi:10.1175/jhm-d-15-0121.1, URL http://dx.doi.org/10.1175/JHM-D-15-0121.1.

Hunt, E. D., K. G. Hubbard, D. A. Wilhite, T. J. Arkebauer, and A. L. Dutcher, 2009: The development and evaluation of a soil moisture index. *International Journal of Climatology*, **29** (**5**), 747–759, doi:10.1002/joc.1749, URL http://dx.doi.org/10.1002/joc.1749.

Kim, D., W. Lee, S. T. Kim, and J. A. Chun, 2019: Historical drought assessment over the contiguous united states using the generalized complementary principle of evapotranspiration. *Water Resources Research*, **55** (**7**), 6244–6267, doi:10.1029/2019wr024991, URL http://dx.doi.org/10.1029/2019WR024991.

Kim, D., and J. Rhee, 2016: A drought index based on actual evapotranspiration from the bouchet hypothesis. *Geophysical Research Letters*, **43** (**19**), 10,277–10,285, doi:10.1002/2016gl070302, URL http://dx.doi.org/10.1002/2016GL070302.

Leasor, Z. T., S. M. Quiring, and M. D. Svoboda, 2020: Utilizing objective drought severity thresholds to improve drought monitoring. *Journal of Applied Meteorology and Climatology*, **59** (**3**), 455–475, doi:10.1175/jamc-d-19-0217.1, URL http://dx.doi.org/10.1175/ JAMC-D-19-0217.1.

Li, J., Z. Wang, X. Wu, C.-Y. Xu, S. Guo, and X. Chen, 2020: Toward monitoring short-term droughts using a novel daily scale, standardized antecedent precipitation evapotranspiration index. *Journal of Hydrometeorology*, **21** (**5**), 891–908, doi:10.1175/jhm-d-19-0298.1, URL http://dx.doi.org/10.1175/JHM-D-19-0298.1.

Liu, Y., Y. Zhu, L. Ren, J. Otkin, E. D. Hunt, X. Yang, F. Yuan, and S. Jiang, 2020: Two different methods for flash drought identification: Comparison of their strengths and

limitations. *Journal of Hydrometeorology*, **21** (**4**), 691–704, doi:10.1175/jhm-d-19-0088.1, URL http://dx.doi.org/10.1175/JHM-D-19-0088.1.

Mahrt, L., and M. Ek, 1984: The influence of atmospheric stability on potential evaporation. *Journal of Climate and Applied Meteorology*, **23** (**2**), 222–234, doi:10.1175/1520-0450(1984)023<0222:tioaso>2.0.co;2, URL http://dx.doi.org/10.1175/ 1520-0450(1984)023<0222:TIOASO>2.0.CO;2.

McEvoy, D. J., J. L. Huntington, M. T. Hobbins, A. Wood, C. Morton, M. Anderson, and C. Hain, 2016: The evaporative demand drought index. Part II: CONUS-wide assessment against common drought indicators. *Journal of Hydrometeorology*, **17** (**6**), 1763–1779, doi:10.1175/jhm-d-15-0122.1, URL http://dx.doi.org/10.1175/JHM-D-15-0122.1.

Mesinger, F., and Coauthors, 2006: North American Regional Reanalysis. *Bulletin of the American Meteorological Society*, **87** (**3**), 343–360, doi:10.1175/bams-87-3-343, URL http: //dx.doi.org/10.1175/BAMS-87-3-343.

National Centers for Environmental Information, 2017: Billion-dollar weather and climate disasters: Overview. URL https://www.ncdc.noaa.gov/billions/.

Noguera, I., F. Domínguez-Castro, and S. M. Vicente-Serrano, 2020: Characteristics and trends of flash droughts in Spain, 1961–2018. *Annals of the New York Academy of Sciences*, **1472** (**1**), 155–172, doi:10.1111/nyas.14365, URL http://dx.doi.org/10.1111/nyas.14365.

Otkin, J. A., M. C. Anderson, C. Hain, I. E. Mladenova, J. B. Basara, and M. Svoboda, 2013: Examining rapid onset drought development using the thermal infrared–based

evaporative stress index. *Journal of Hydrometeorology*, **14** (**4**), 1057–1074, doi:10.1175/jhm-d-12-0144. 1, URL http://dx.doi.org/10.1175/JHM-D-12-0144.1.

Otkin, J. A., M. C. Anderson, C. Hain, and M. Svoboda, 2014: Examining the relationship between drought development and rapid changes in the evaporative stress index. *Journal of Hydrometeorology*, **15** (**3**), 938–956, doi:10.1175/jhm-d-13-0110.1, URL http://dx.doi.org/10.1175/JHM-D-13-0110.1.

Otkin, J. A., M. Shafer, M. Svoboda, B. Wardlow, M. C. Anderson, C. Hain, and J. Basara, 2015: Facilitating the use of drought early warning information through interactions with agricultural stakeholders. *Bulletin of the American Meteorological Society*, **96** (**7**), 1073–1078, doi:10.1175/bams-d-14-00219.1, URL http://dx.doi.org/10.1175/ BAMS-D-14-00219.1.

Otkin, J. A., M. Svoboda, E. D. Hunt, T. W. Ford, M. C. Anderson, C. Hain, and J. B. Basara, 2018: Flash droughts: A review and assessment of the challenges imposed by rapid-onset droughts in the united states. *Bulletin of the American Meteorological Society*, **99** (**5**), 911–919, doi:10.1175/bams-d-17-0149.1, URL http://dx.doi.org/10.1175/ BAMS-D-17-0149.1.

Otkin, J. A., Y. Zhong, E. D. Hunt, J. Basara, M. Svoboda, M. C. Anderson, and C. Hain, 2019: Assessing the evolution of soil moisture and vegetation conditions during a flash drought–flash recovery sequence over the south-central united states. *Journal of Hydrometeorology*, **20** (**3**), 549–562, doi:10.1175/jhm-d-18-0171.1, URL http://dx.doi.org/10.1175/JHM-D-18-0171.1.

Pachauri, R. K., and Coauthors, 2014: Climate Change 2014: Synthesis Report. Contribution of Working Groups I, II and III to the Fifth Assessment Report of the Intergovernmental Panel on Climate Change. IPCC, Geneva, Switzerland.

Svoboda, M., and Coauthors, 2002: The drought monitor. *Bulletin of the American Meteorological Society*, **83** (**8**), 1181–1190, doi:10.1175/1520-0477-83.8.1181, URL http: //dx.doi.org/10.1175/1520-0477-83.8.1181.

Vicente-Serrano, S. M., and Coauthors, 2018: Global assessment of the standardized evapotranspiration deficit index (SEDI) for drought analysis and monitoring. *Journal of Climate*, **31** (**14**), 5371–5393, doi:10.1175/jcli-d-17-0775.1, URL http://dx.doi.org/10.1175/JCLI-D-17-0775.1.

Wakefield, R. A., J. B. Basara, J. C. Furtado, B. G. Illston, C. R. Ferguson, and P. Klein, 2019: A modified framework for quantifying land–atmosphere covariability during hydrometeorological and soil wetness extremes in Oklahoma. *Journal of Applied Meteorology and Climatology*, **58** (**7**), 1465–1483, doi:10.1175/jamc-d-18-0230.1, URL http://dx.doi.org/10.1175/JAMC-D-18-0230.1.

Supplementary Figures

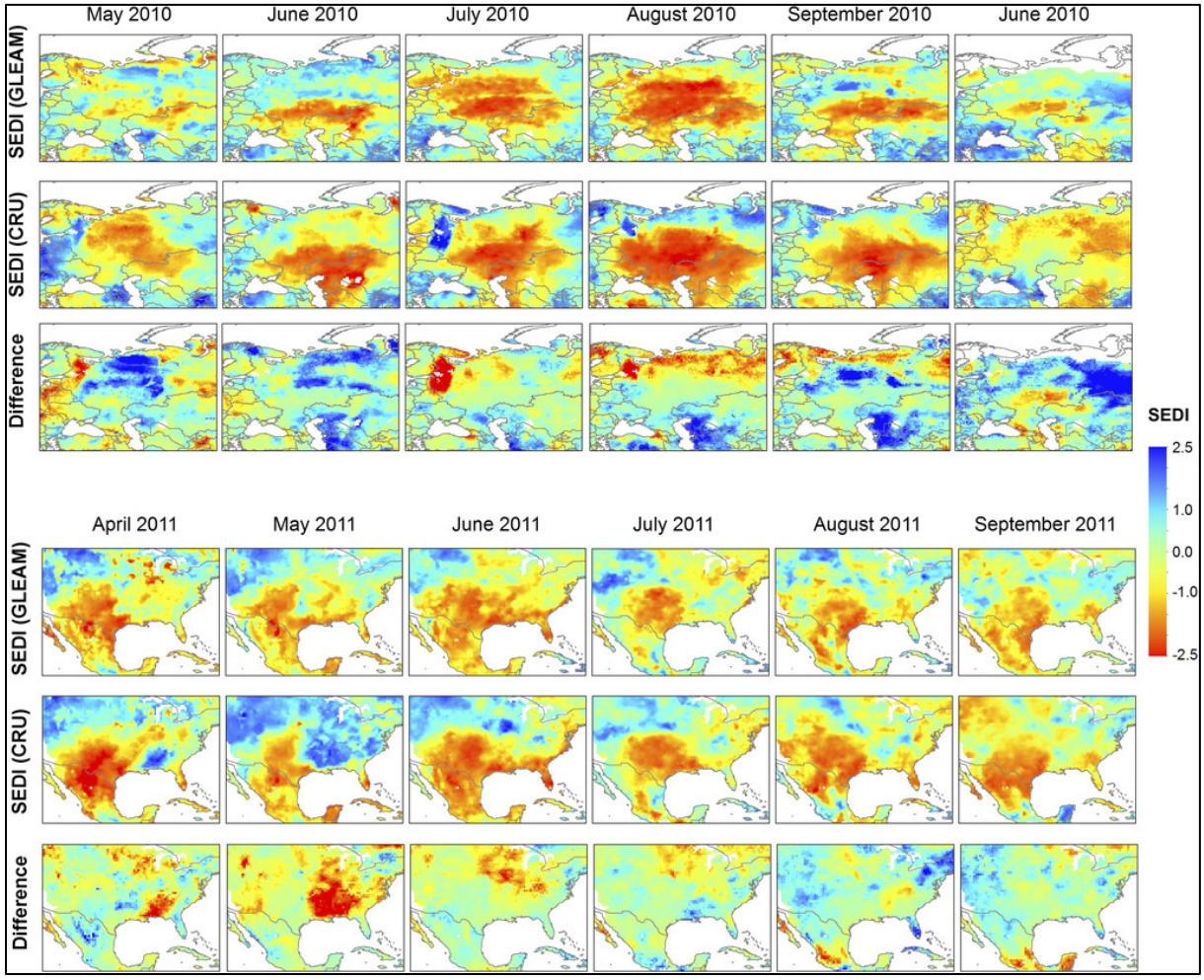

Supplementary Figure 1. SEDI distribution for Russia 2010 (top) and North America 2011 (Bottom). [Figure and caption from Figure 5 in Vicente-Serrano et al. (2018).]

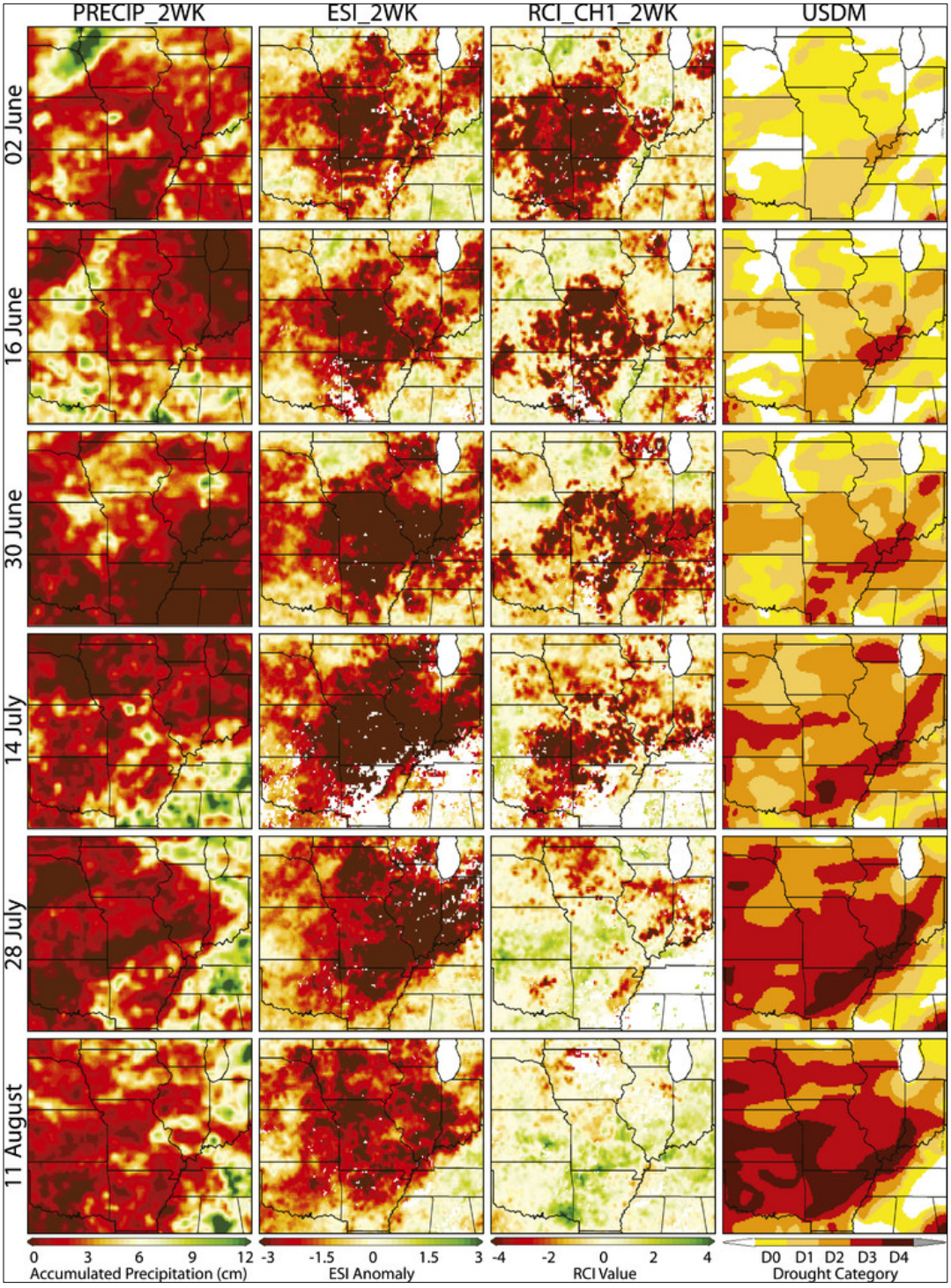

Supplementary Figure 2. Temporal evolution of 2-week accumulated precipitation, ESI, RCI, and USDM drought depiction from 2 Jun to 11 Aug 2012. [Figure and caption from Figure 2 in Otkin et al. (2014).]

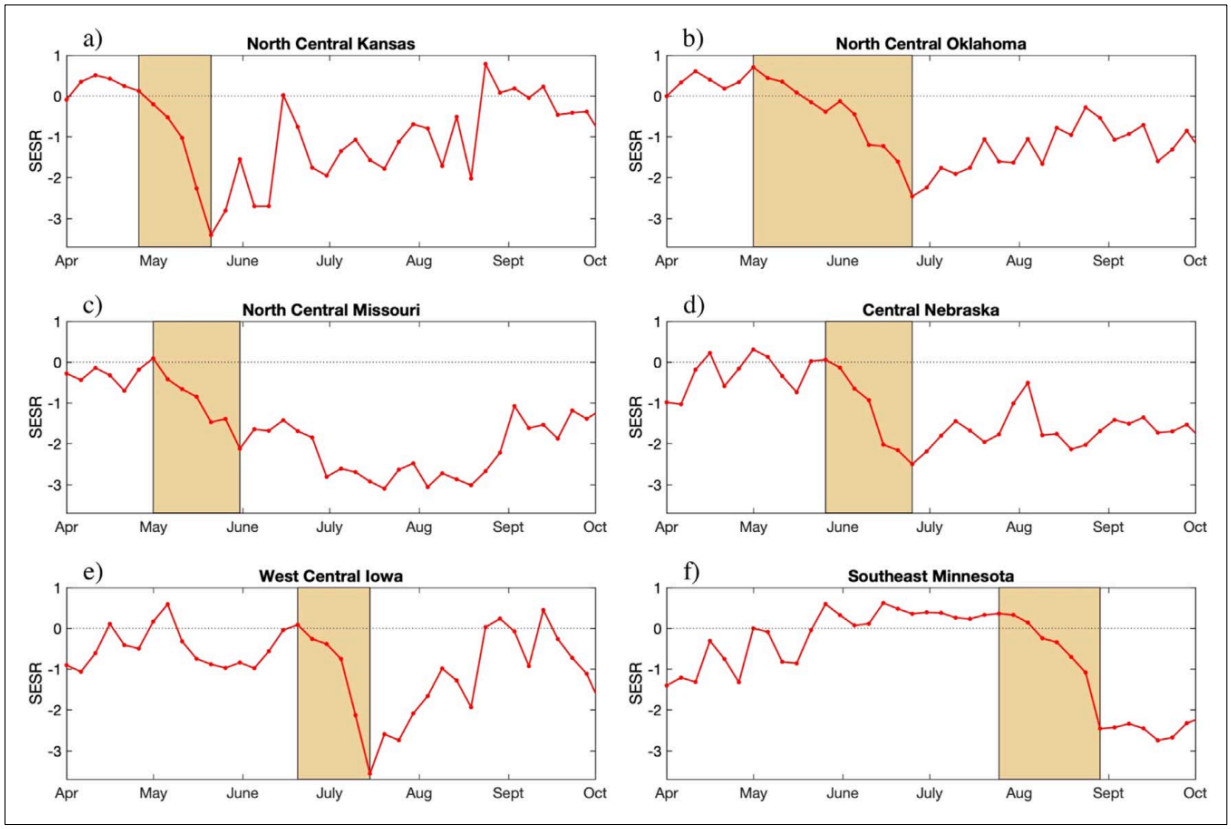

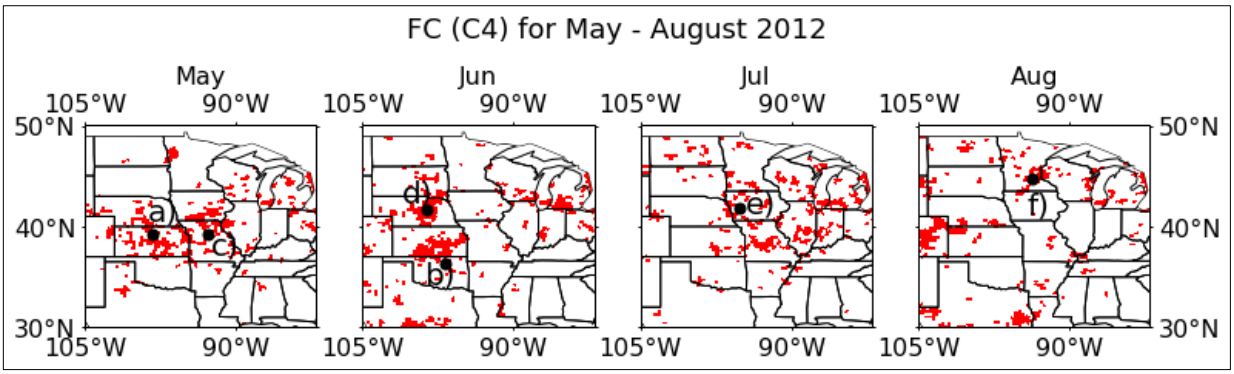

Supplementary Figure 3. (top) SESR (red line) from the NARR dataset for six locations across the Great Plains and Midwest. The shaded tan region on each panel represents the temporal period for flash drought from the flash drought identification methodology. (bottom) Rapid intensification for the growing season in 2012 with points from the time series highlighted. [Figure and caption from Figure 4 in Basara et al. (2019).]

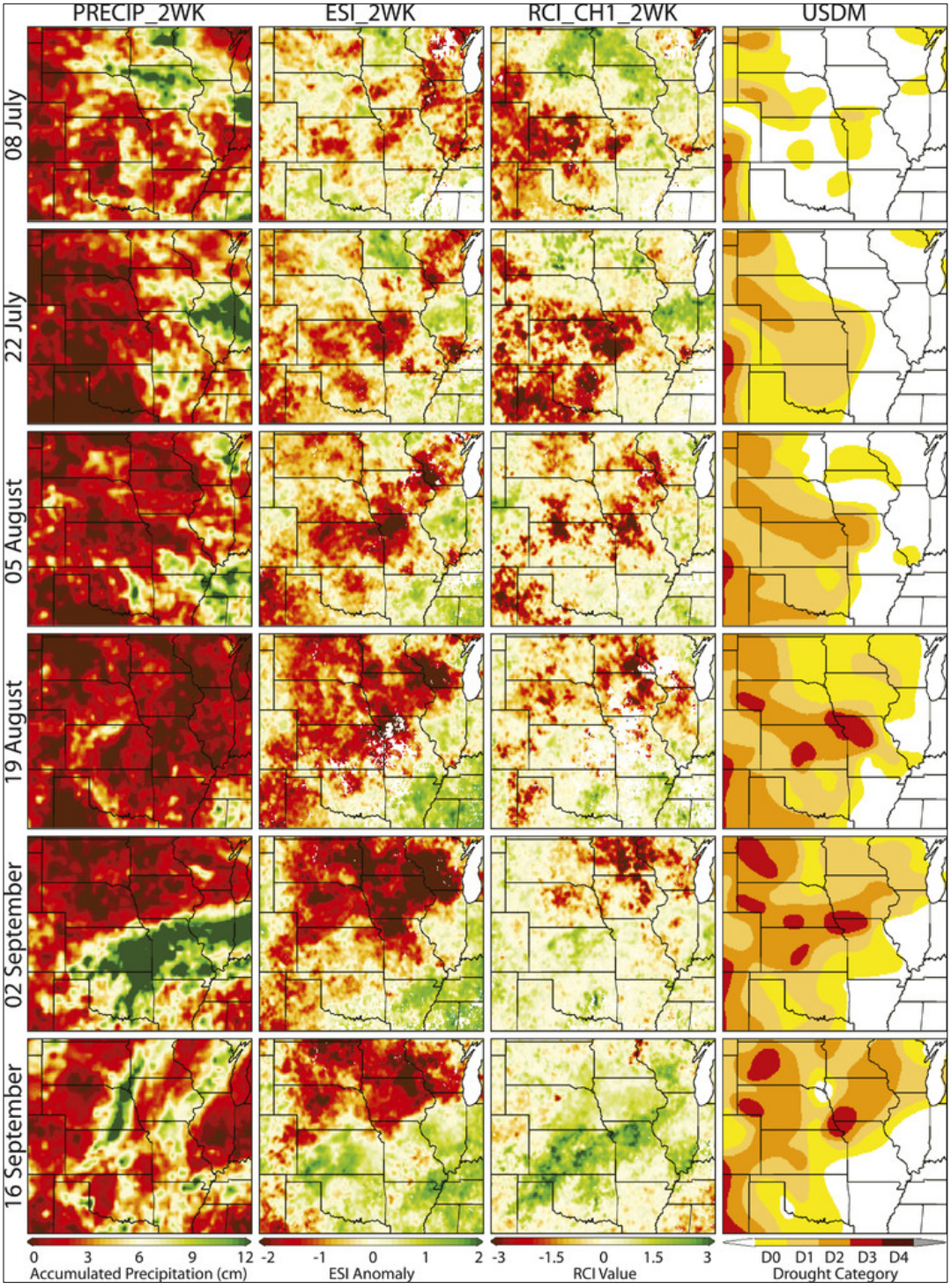

Supplementary Figure 4. Temporal evolution of 2-week accumulated precipitation, ESI, RCI, and USDM drought depiction from 8 Jul to 16 Sep 2003. [Figure and caption from Figure 1 in Otkin et al. (2014).]